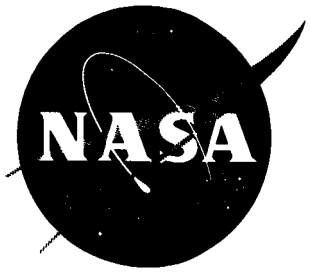

TECHNICAL NOTE

D-4

INFLUENCE OF SHAFT DEFLECTION AND SURFACE ROUGHNESS ON LOAD-CARRYING CAPACITY OF PLAIN JOURNAL BEARINGS

By F. H. Raven and R. L. Wehe
Cornell University

NATIONAL AERONAUTICS AND SPACE ADMINISTRATION
WASHINGTON
August 1959

NATIONAL AERONAUTICS AND SPACE ADMINISTRATION

TECHNICAL NOTE D-4

INFLUENCE OF SHAFT DEFLECTION AND SURFACE ROUGHNESS ON LOAD-CARRYING CAPACITY OF PLAIN JOURNAL BEARINGS

By F. H. Raven and R. L. Wehe

SUMMARY

Shaft deflection is one of the many factors known to limit the load capacity of full journal bearings to magnitudes less than the infinite value predicted by hydrodynamic theory. This deflection produces an adverse alinement of journal and bearing that causes metal contact at the bearing ends and subsequent failure by seizure. The analysis presented herein, together with experimental data, shows that the load capacity of a bearing with flexible shaft may be predicted to a reasonable order of magnitude. Shaft deflection and roughness of the bearing surfaces are shown to be factors of first-order importance in limiting the load capacities of bearings. On the basis of the criteria presented, it is shown that the optimum length-diameter ratio of a bearing is reasonably predictable.

INTRODUCTION

The purpose of this report is to set forth a criterion that includes shaft deflection for estimating the maximum load capacity of full journal bearings. Hydrodynamic theory for journal bearings predicts an infinite load capacity as the oil film thickness approaches zero. However, analytical approximations in this theory do not include the effect of elastic deflection of the journal that becomes of the order of magnitude of the film thickness as the load increases.

In heavily loaded bearings, metallic contact of the journal and bearing occurs at some local point, usually at the ends of a bearing, because of elastic deflection of the shaft. Figure 1 shows two typical cases of the attitude of a deflected shaft in the bearing, one being a central bearing where the curvature of the journal causes a reduced film thickness at the two ends of the bearing, and the other being an end bearing where the slope of the deflected shaft causes a reduced film at the inboard end of the bearing.

According to hydrodynamic theory, an ideally straight shaft under load is displaced in the bearing clearance as shown in figure 2. The hydrodynamic displacement e is in a direction given by the attitude angle φ; but for a flexible shaft the elastic deflection within the bearing length is parallel to the direction of the load such that the attitude angle φ_E at the end of the bearing is less than φ.

Failure does not necessarily occur when local metallic contact between the journal and bearing first takes place. Because of the conformability of certain bearing materials, bearings that have been carefully run in may operate satisfactorily even though metallic contact geometrically appears to exist over some length l' near the ends of the bearing as shown in figure 3. As run-in proceeds with only local heating effects, increases in l' give increases in mean eccentricity ratio and corresponding increases in hydrodynamic load capacity.

It should be noted that the misalining effect of the slope of the elastic curve of a flexible shaft in an end bearing could be eliminated by either a self-alining bearing support or by matching the elastic slope of the bearing mounting with that of the shaft. The purpose of this report is to evaluate the effect on load capacity when this improvement is not provided. Since the shaft is usually much more flexible than the bearing support, the words shaft stiffness or shaft deflection are used herein to refer to the displacement caused by the difference in alinement of the bearing and the journal. With perfect alinement and zero curvature of the journal the minimum film thickness is limited by surface roughness.

Thus, the geometric relations of journal and bearing in figures 1 and 2 indicate that the load capacity of a bearing depends on: (1) hydrodynamic relations, (2) shaft stiffness, (3) bearing length-diameter (l/d) ratio, and (4) roughness of the bearing surfaces. For an ideally rigid shaft and ideally smooth bearing surfaces, the load capacity of a bearing is infinite. The load capacity is reduced to some finite value if the metallic contact of the surface asperities due to surface roughness breaks through the oil film to produce high friction and a prohibitive temperature rise. If the shaft has relatively great flexibility, metallic contact at a local point limits the load capacity, and surface roughness has a lesser limiting influence. For a flexible shaft, the bearing length-diameter ratio also has an important effect, since long bearings are less able to accommodate a sloping shaft. As a bearing becomes shorter, the effect of shaft deflection within the bearing length is reduced, and a higher mean eccentricity is given; but at the same time a shorter length reduces load capacity hydrodynamically.

In this report the load capacity of a bearing with flexible shaft is evaluated mathematically by using the criterion of first local metallic contact. Charts usable in design, which in dimensionless form show load

capacity as a function of length-diameter ratio with certain shaft stiffness factors as parameters, are presented. A method of determining the optimum l/d ratio of a bearing for maximum load capacity, based both on shaft deflection and bearing surface roughness, is given.

The hydrodynamic relations on which the following analysis depends are those given by the short-bearing approximation (ref. 1) and those determined experimentally (ref. 2). The relations concerned with shaft deflection are those for a simply supported beam and a cantilever beam and include the effect of elastic curvature on center bearings and the effect of elastic slope on end bearings.

Analytical calculations of bearing load capacity based on shaft deflection are compared with the capacities obtained experimentally by the Battelle Memorial Institute and are shown to be of equal order of magnitude. Experimental curves presented by Falz and by Deck show the dependence of bearing load capacity on l/d ratio. Curves obtained analytically are similar in form and show an optimum l/d.

This investigation was conducted by the bearing research group in the Department of Machine Design, Sibley School of Mechanical Engineering, Cornell University, Ithaca, New York, under the sponsorship and with the financial aid of the National Advisory Committee for Aeronautics.

SYMBOLS

A	deflection-eccentricity ratio, $k\delta/e$
a,b	distance between center bearing and end bearing, in.
l/C_n	load number for l/d less than 1.0, $\frac{p}{\mu N}\left(\frac{c_d}{d}\right)^2\left(\frac{d}{l}\right)^2$
c_d	diametral bearing clearance, in.
c_d/d	clearance ratio
c_r	radial bearing clearance, $c_d/2$, in.
d	bearing diameter, in.
E	modulus of elasticity, psi
e	mean eccentricity or mean hydrodynamic displacement, in.
h_E	end minimum film thickness, in.

h_{min}	mean minimum film thickness, in.
I	moment of inertia of cross section of beam, $in.^4$
K	beam stiffness parameter
k	coefficient denoting fraction of δ
L	beam length, in.
l	bearing length, in.
l'	length of contact at end of run-in bearing, in.
l/d	bearing length-diameter ratio
N	journal speed, rps
n	eccentricity ratio, e/c_r
P	total bearing load, lb
p	unit bearing load on projected area, psi
R	load-spacing - beam-length ratio, a/L, b/L
r	beam-length - bearing-length ratio, L/l
S	Sommerfeld number, $\frac{\mu N}{p}\left(\frac{d}{c_d}\right)^2$
l/S	load number for l/d greater than 1.0
x,y	coordinates of beam elastic curve, in.
β	slope of elastic curve at end of beam, radian
Δ	ratio of error in h_E to radial clearance c_r
δ	deflection of journal within bearing length, in.
μ	fluid viscosity, $\frac{\text{centipoises}}{6.9\times10^6}$, reyns
φ	mean attitude angle between load line and line of centers, deg
φ_E	attitude angle at end of bearing, deg

ANALYSIS

When the effect of elastic bending of the shaft on bearing load capacity is analyzed, the fact should be recognized that, even if the journal remains essentially parallel to the bearing as in figure 1(b), the elastic curvature within the length of the bearing is appreciable. The local minimum film thickness h_E at the end of the bearing is considerably less than h_{min}, which represents the idealized minimum film thickness of a theoretically straight journal parallel to its bearing.

Figure 1(b), which shows the elastic curve of a center bearing, illustrates that the journal has a different eccentricity at each point along its length. It should be recognized that the center of the shaft at the central transverse plane of the bearing will not necessarily be at the idealized hydrodynamic displacement h_{min}. Thus, the difference between h_E and h_{min} depends on: (1) the effect of the elastic curvature on the idealized hydrodynamic displacement, and (2) the shape of the elastic curve. Since both (1) and (2) are related to the elastic curvature, mathematically the difference between h_{min} and h_E can be expressed by a quantity k times the elastic deflection δ within the bearing length:

$$h_{min} - h_E = k\delta \tag{1a}$$

In this form the value of k remains to be determined, but it is evident that a real value of k exists for any particular bending configuration and operating condition. Experimental measurement of film thickness at any point within the bearing length is difficult; and analytical methods become involved with a two-dimensional solution of Reynolds' equation, in which the pressure distribution affects the shape of the elastic curve.

With the concept of a mean eccentricity e represented by the straight line in figure 1(b), it seems reasonable to assume that the difference between h_E and the mean line is less than the height of the elastic curve or that $k < 1$. However, equation (1a) holds without making this assumption.

Since exact evaluation of k for a particular configuration is difficult, an approximation of the value of k seems desirable. Perhaps the simplest approximation for a center bearing (fig. 1(b)) is to assume a uniformly distributed load on the beam; this gives an elastic curve in the form of a fourth-degree parabola, for which the arithmetic mean occurs at $\frac{4}{5}\delta$. Thus, the center of the elastic curve is $\frac{1}{5}\delta$ away from the

mean line, and the difference between h_{min} and h_E is 0.8 δ, which gives an approximate value of $k = 0.8$ for a center bearing. This approximation was found to be of value in reducing the spread of experimental measurements of eccentricity in previous investigations (refs. 1 and 2).

Figures 1(c) and 2 show the elastic slope or tilt of the journal axis in a bearing at the end of a shaft. The end of a shaft, considered as part of a beam, represents a point where the bending moment is zero and the elastic slope is large. Experiments on misalined bearings (ref. 3) have shown that, to a first approximation, the eccentricity e at the central transverse plane of the bearing under a constant load remains essentially fixed as the journal is misalined by a couple that inclines the journal axis. In effect, the central point acts like a pivot point. Thus, the hydrodynamic load on a misalined or inclined journal may be approximated to be the same as the load on a theoretically straight and parallel shaft passing through the pivot point. This concept enables the eccentricity of the center of an inclined journal to be estimated from hydrodynamic data for a straight and parallel shaft. In figure 1(c), the bending moment is small and the journal is essentially straight, but inclined. Thus, the deflection δ, from the pivot point may be estimated as the slope times $l/2$, where $l/2$ is the half-length of the bearing. Thus, for an end bearing the value of k is one to a first approximation.

Thus, the value of k may be determined to varying degrees of approximation. However, in general, from equation (1a), the difference between h_{min} and h_E is $k\delta$, where k is an arbitrary coefficient. Solving for h_E gives

$$h_E = h_{min} - k\delta \tag{1b}$$

Equation (1b) is realistic only when the attitude angle φ shown in figure 2 is equal to zero. However, when φ is other than zero, the determination of h_E depends also on attitude angle as well as on the variables of equation (1b). As shown by the triangles appearing in the clearance circle of figure 2, an approximate expression involving attitude angle is:

$$h_{min} - h_E = k\delta \cos \varphi$$

$$h_E = h_{min} - k\delta \cos \varphi \tag{2}$$

At conditions near metallic contact, the attitude angle is small and the cosine of the angle is near unity. Conservatively, $\cos \varphi = 1.0$ could be used; but when $\varphi = 20^{\circ}$ is assumed to be an average value in the heavily loaded region, equation (2) becomes

$$h_E = h_{min} - 0.94\, k\delta \tag{3}$$

Appendix A gives an analysis of the errors involved in the approximations of equations (2) and (3) to show that the approximations are reasonable.

Mean Minimum Film Thickness

In order to use equation (3), it is necessary to evaluate h_{min} and δ. The mean minimum film thickness h_{min} involves the hydrodynamic variables including load and may be evaluated from hydrodynamic theory. According to the short-bearing approximation (ref. 1), the mean eccentricity e under hydrodynamic conditions is given by the curve of figure 4 in which eccentricity ratio $n = e/c_r$ is plotted against the bearing variables appearing in the load number. In reference 4, the equation of this curve is rearranged so that the minimum film thickness h_{min} rather than the diametral clearance c_d is included in the bearing variables as a function of eccentricity ratio:

$$\frac{p}{\mu N}\left(\frac{h_{min}}{l}\right)^2 = \frac{\pi}{4}\frac{n}{(1+n)^2}\left[\pi^2(1-n^2) + 16n^2\right]^{1/2}$$

$$= f(n)$$

where μ is the film viscosity, N is journal speed in rps, l is bearing length, and p is the unit load determined from the load P divided by ld. Rearranging equation (4) gives

$$\frac{h_{min}}{l} = \sqrt{\frac{\mu N}{p}}\sqrt{f(n)} \qquad (\text{for } l/d \leq 1.0) \tag{5}$$

Experiment (ref. 2) has shown that the short-bearing approximation is reasonable for short bearings with length-diameter ratios equal to or less than 1.0. Also, in reference 2, experiment shows that the short-bearing solution approximates the behavior of longer bearings if a modification in the l/d term is made. In the form of equation (5), the mean minimum-film-thickness function for bearings of $l/d > 1.0$ is given as follows:

$$\frac{h_{min}}{l} = \frac{\sqrt{\mu N/p}}{l/d}\sqrt{f(n)} \qquad (\text{for } l/d \geq 1.0) \tag{6}$$

Numerical evaluation of the function $f(n)$ in equation (4) shows that for values of n from 0.6 to 1.0 the function changes from 0.640 to 0.785. By assuming that most bearings will be heavily loaded at an eccentricity ratio in excess of $n = 0.6$, the variation of $f(n)$ will not be great. By selecting a mean eccentricity ratio of 0.8 and the corresponding value of $f(n) = 0.718$, the maximum variation in $f(n)$ is approximately 10 percent. Since the minimum film thickness h_{min} depends on the square root of $f(n)$ or 0.848, the maximum variation in h_{min} is of the order of 5 percent. The following simplified expressions result:

$$\frac{h_{min}}{l} = 0.848 \sqrt{\frac{\mu N}{p}} \qquad (\text{for } l/d \leqq 1.0) \qquad (7a)$$

$$\frac{h_{min}}{l} = 0.848 \frac{\sqrt{\mu N/p}}{l/d} \qquad (\text{for } l/d \geqq 1.0) \qquad (7b)$$

To investigate further the error of assuming a constant $f(n) = 0.718$ for heavily loaded bearings, equation (7a) may be rearranged to give the equation of eccentricity ratio n as a function of load number and may be plotted in figure 4. By substituting $h_{min} = (c_d/2)(1 - n)$ in equation (7a), the following equation results:

$$\frac{p}{\mu N}\left(\frac{c_d}{d}\right)^2\left(\frac{d}{l}\right)^2 = \frac{2.85}{(1 - n)^2} \qquad (8)$$

Plotting this equation on the coordinates of figure 4 indicates that the curve is almost indistinguishable from the exact curve given by the short-bearing approximation in the range of $n \geqq 0.6$.

By using the simplified equations (7) and substituting them in equation (3), the equations for determining the minimum end clearance h_E appear as follows:

$$\frac{h_E}{l} = 0.848 \sqrt{\frac{\mu N}{p}} - 0.94 \frac{k\delta}{l} \qquad (\text{for } l/d \leqq 1.0) \qquad (9a)$$

$$\frac{h_E}{l} = 0.848 \frac{\sqrt{\mu N/p}}{l/d} - 0.94 \frac{k\delta}{l} \qquad (\text{for } l/d \geqq 1.0) \qquad (9b)$$

If the viscosity, journal speed, load, and bearing length and diameter are known and the deflection δ within the length of the bearing is calculable, the dimension of the thinnest point in the film may be determined from equations (9). To facilitate the calculations, these equations are plotted in figure 5 and are in a form usable in design.

In the foregoing, the hydrodynamic part of the analysis is based on the numerical values obtained from the equations of the short-bearing approximation. However, experimental measurements of eccentricity (ref. 2) differ somewhat from the analytical values as shown in figure 4. For example, for a load number of 75, the analytical value of n is 0.80 and the experimental value is 0.92. The film thickness is proportional to $(1 - n)$, which is 0.20 corresponding to $n = 0.80$, and 0.08 corresponding to $n = 0.92$. This illustrates the greater sensitivity obtained by using film thickness as the variable, since the difference is apparently increased. Therefore, it would be conservative to base the bearing load capacity on the experimental curve of figure 4 since the load capacity is less. A curve drawn through part of the experimental data in figure 4 is obtained by using an average value of $f(n) = 0.30$ instead of 0.718 and approximates the curve of experimental data in the range of $n = 0.6$ to 0.85. In the range higher than $n = 0.85$, a value of $f(n)$ less than 0.30 would be desirable to approximate the experimental data better. Based on $f(n) = 0.30$, the equations comparable to equations (9) are:

$$\frac{h_E}{l} = 0.546 \sqrt{\frac{\mu N}{p}} - 0.94 \frac{k\delta}{l} \qquad (\text{for } l/d \leqq 1.0) \qquad (10a)$$

$$\frac{h_E}{l} = 0.546 \frac{\sqrt{\mu N/p}}{l/d} - 0.94 \frac{k\delta}{l} \qquad (\text{for } l/d \geqq 1.0) \qquad (10b)$$

In figure 5 are shown the curves for predicting h_E from equations (10) for comparison with those from equations (9). As may be seen, the end minimum film thicknesses are smaller where the experimental hydrodynamic characteristics are used.

Maximum Load Capacity

A convenient and obvious design criterion is that the load capacity of a bearing is a maximum when h_E is zero and the bearing surfaces are in contact at a point. When the film thickness at the end of the bearing is zero, the mean eccentricity generally will be greater than 0.6 for reasonable stiffnesses of shaft. Therefore, when h_E equals zero, equations (9) reduce to the following expressions:

$$\frac{p}{\mu N} = 0.81 \left(\frac{l}{k\delta}\right)^2 \qquad (\text{for } l/d \leqq 1.0) \qquad (11a)$$

$$\frac{p}{\mu N} \left(\frac{l}{d}\right)^2 = 0.81 \left(\frac{l}{k\delta}\right)^2 \qquad (\text{for } l/d \geqq 1.0) \qquad (11b)$$

Thus, figure 6 shows that the maximum load capacity depends on the square of the deflection δ; this indicates a rapid rise in load capacity as the stiffness of the shaft is increased. Also, equations (11) show an infinite load capacity for an ideally rigid shaft where δ is zero.

The corresponding equations where the experimental hydrodynamic data are used are the same as equations (11) except that the coefficient is 0.34 instead of 0.81. Therefore, the load capacity based on experimental hydrodynamic data is approximately 40 percent of the capacity based on the short-bearing solution. Figure 6 shows the comparison of load capacities of the two cases.

Evaluation of Deflection δ

Either of the two curves of figure 6 is a simple basic curve giving the maximum load capacity of a bearing with a flexible shaft. However, it is assumed that the deflection δ within the length of the bearing can be computed by analytical or graphical means. This in many instances may be a complicated but possible process, since the theory of beam deflection is well developed. The major complication is that, if the maximum load of the bearing is to be determined, it is necessary to know the load to determine the deflection δ, so that a trial and error solution may be necessary. However, for certain elementary cases of beam loadings, calculations of δ are readily made by mathematical means as illustrated in the following paragraphs.

Two types of beams are considered: (1) a simply supported beam with offcenter or unsymmetrical load as shown in figure 7, and (2) a cantilever beam as shown in figure 8. The bearings shown are of two classes: end bearings where δ depends on the slope of the ends of the beam, and central bearings where δ is dependent on the local curvature of the bent beam and to some extent on the slope of the elastic curve. Of the two classes of bearings, the end bearing is subject to a greater δ and will have the lower load capacity. For the end bearings, the calculation of δ depends only on the slope β of the beam times the half-length $l/2$ of the bearing.

Deflection of End Bearings

For the simply supported beam of figure 7, the left end bearing has the greater slope β_1, since it is nearest the applied load P. From deflection formulas,

$$\beta_1 = \frac{Pb}{6LEI}\left(L^2 - b^2\right) \qquad (12)$$

The unit pressure loading on the left end bearing may be expressed in terms of the applied central load P as follows:

$$p = \frac{b}{L}\frac{P}{ld} \tag{13}$$

By substituting this expression in equation (12) and letting $I = \pi d^4/64$, $r = L/l$, and $R = b/L$, the following expression for β_1 is obtained:

$$\beta_1 = \frac{32}{3\pi}\frac{p}{E}\left(\frac{l}{d}\right)^3 r^2 (1 - R^2) \tag{14}$$

The deflection δ may be obtained from:

$$\delta = \beta_1 \, l/2$$

$$= \frac{16pl}{3\pi E}\left(\frac{l}{d}\right)^3 r^2 (1 - R^2)$$

$$= \frac{4}{\pi}\frac{pl}{E}\left(\frac{l}{d}\right)^3 1.33r^2 (1 - R^2)$$

$$\delta = \left[\frac{4}{\pi}\frac{pl}{E}\left(\frac{l}{d}\right)^3\right]K \tag{15}$$

As shown in subsequent paragraphs, the quantities in the brackets of equation (15) appear regularly for many cases of beam loading so that K is the distinguishing quantity for the deflection of the many cases.

By substituting equation (15) for δ in equations (11) for load capacity, the following equations are obtained with $k = 1.0$ for end bearings:

$$\frac{p}{\mu N}\left(\frac{p}{E}\right)^2 = \left[\frac{0.71}{K(l/d)^3}\right]^2 \qquad (\text{for } l/d \leqq 1.0) \tag{16a}$$

$$\frac{p}{\mu N}\left(\frac{p}{E}\right)^2 = \left[\frac{0.71}{K(l/d)^4}\right]^2 \qquad (\text{for } l/d \geqq 1.0) \tag{16b}$$

where

$$K = 1.33\, r^2 (1 - R^2) = 1.33\left(\frac{L}{l}\right)^2\left[1 - \left(\frac{b}{L}\right)^2\right] \tag{17}$$

Equations (16) show that the unit load capacity of an end bearing is greatly influenced by l/d ratio. As shown in the curves of equations (16) plotted in figure 9(a), the unit load capacity increases by decreasing l/d for a given value of the stiffness parameter K. However, this is somewhat misleading if a reduction of l/d is made by decreasing the bearing length l, since the bearing length is also included in K; although for a given design the influence of K would be less than that of l/d. If a reduction in l/d is made by increasing the diameter d, K is unaffected and the increase in load capacity is predicted according to the curves of figure 9(a).

Figure 9(b) is similar to 9(a) except that the numerical values are based on the hydrodynamic data determined experimentally, so that the coefficient in equations (16) is 0.46 instead of 0.71; this gives more conservative values of load capacity.

The bearing of the cantilever beam shown in figure 8 is also an end bearing. Since the beam is different from the simply supported beam of figure 7, the resultant formula for δ is also different. However, equations (16) and the curves of figure 9 also apply to this bearing if $K = 4r^2$ is used. The determination of δ for the bearing of the cantilever beam is shown in appendix B.

Total Load Capacity of an End Bearing

The total load P that will just cause metallic contact to take place is readily determined by multiplying the unit bearing pressure p as determined in equations (16) by the projected bearing area ld. By substituting $p = P/ld$ in equations (16) and using the expression for K in equation (17), the following equations are derived for the end bearing of the simply supported beam of figure 7:

$$\frac{P}{(\mu N E^2)^{1/3}} \left(\frac{L}{d}\right)^{4/3} \left(\frac{l}{d}\right)^2 = \frac{0.658}{(1 - R^2)^{2/3}} \left(\frac{l}{d}\right)^{1/3} \qquad (\text{for } l/d \leqq 1.0) \tag{18a}$$

$$\frac{P}{(\mu N E^2)^{1/3}} \left(\frac{L}{d}\right)^{4/3} \left(\frac{l}{d}\right)^2 = \frac{0.658}{(1 - R^2)^{2/3}} \frac{1}{(l/d)^{1/3}} \qquad (\text{for } l/d \geqq 1.0) \tag{18b}$$

In dimensionless form, equations (18) give the total load capacity of an end bearing as a function of l/d. The dependence of load capacity on l/d is shown in the family of curves in figure 10(a). The parameter R indicates the influence of the location along the beam of the applied load; for a centrally placed load, R is equal to 0.5.

The variation of the total load capacity of an end bearing with change in bearing length is readily determined from figure 10(a); that is, if all the bearing variables are held constant except l, the curves are a graphical representation of the variation of bearing capacity with length alone. The maximum load capacity is obtained when the bearing length is equal to its diameter. As the length becomes larger than the diameter, the capacity decreases because the increased effect of journal deflection does not permit the bearing to run at a higher mean eccentricity. As the length becomes less than the diameter, the bearing operates at a higher mean eccentricity; but the decrease of projected area of the bearing lowers the total capacity.

Figure 10(a) also gives the curve for the total load capacity of an end bearing of the cantilever beam of figure 8. Equations for this bearing are similar to equations (18), since they are also derived from equations (16), except that $K = 4r^2$. The dependence on l/d of this bearing is somewhat different as shown by the equations in appendix C.

A companion set of curves giving numerical values of total load capacity based on the experimental hydrodynamic data with $f(n) = 0.30$ are shown in figure 10(b). Equations (18) apply except that the coefficient is 0.492 instead of 0.658 for end bearings of the simply supported beam.

Although equations (18) and figure 10 indicate that highest load capacity is obtained at $l/d = 1.0$, this is true only if l/d depends on a change in length. If the diameter d is changed instead, then the effect on load capacity is not obvious from the curves. However, it is possible to rearrange equations (18) so that l instead of d appears in the left term.

$$\frac{P}{(\mu N E^2)^{1/3}} \left(\frac{L}{l}\right)^{4/3} \left(\frac{l}{l}\right)^2 = \frac{0.658}{(1 - R^2)^{2/3}} \frac{1}{(l/d)^3} \qquad (\text{for } l/d \leqq 1.0) \tag{19a}$$

$$\frac{P}{(\mu N E^2)^{1/3}} \left(\frac{L}{l}\right)^{4/3} \left(\frac{l}{l}\right)^2 = \frac{0.658}{(1 - R^2)^{2/3}} \frac{1}{(l/d)^{11/3}} \qquad (\text{for } l/d \geqq 1.0) \tag{19b}$$

The curves of equations (19) are shown in figures 11(a) and 11(b), the former set of curves depending on the analytical hydrodynamic data and the latter on the experimental data.

If all bearing parameters other than diameter are kept constant, the total load capacity increases rather sharply as the diameter is increased, as may be seen from the curves of figure 11. As l/d is made to approach zero by increasing the diameter, the load capacity approaches an infinite value because the shaft stiffness is increased greatly by diameter increase to permit the bearing to operate at a higher mean eccentricity before metallic contact takes place.

The equations that apply to the end bearing of the cantilever beam are shown in appendix C.

Unit Load Capacity of a Central Bearing

If the inboard bearing of the simply supported beam of figure 7 is considered, the calculation of δ is most easily made when the bearing is located at the center of the beam. The deflection of the beam at its center is y_{max} and coincides with the transverse central plane of the bearing. Deflection formulas, as shown in appendix D, may be used to determine the beam deflection y_{max} and also the deflection y_E at the end of the bearing. As shown in figure 1(c), the deflection δ within the half-length of the bearing is the difference of the two beam deflections:

$$\delta = y_{max} - y_E \tag{20}$$

As shown in appendix D, the resultant equation for δ is expressed as follows:

$$\delta = \left[\frac{4}{\pi}\frac{pl}{E}\left(\frac{l}{d}\right)^3\right]0.167\,(3r - 1) \tag{21}$$

When this expression is substituted in equations (11) and $k = 0.8$ is used, the equations obtained are the same as equations (16) except that the stiffness factor is $K = 0.133\,(3r - 1)$. It is observed that K includes k in this case. Thus, the unit load capacity curves of figure 9 may be used generally for both end bearings and central bearings except that the proper K values must be used as indicated in the figures. A comparison of K values shows that the unit load capacity of a central bearing is greater than an end bearing if all variables except K are assumed constant in equations (16).

$$\frac{p_{central}}{p_{end}} = \left(\frac{K_{end}}{K_{central}}\right)^{2/3} \tag{22}$$

For a simply supported beam with the central bearing located at the beam center, the ratio of the unit load capacities of the two bearings is

$$\frac{p_{central}}{p_{end}} = \left[\frac{7.5 \left(\frac{L}{l}\right)^2}{3\,L/l - 1}\right]^{2/3} \tag{23}$$

If for illustration the length of the beam L is assumed five times greater than the bearing length l, then

$$\frac{p_{central}}{p_{end}} = 5.65$$

The ratio of load capacities is sensitive to L/l as equation (23) indicates and thus decreases as the end and center bearings are brought together by decreasing the beam length L. Increasing the beam length, on the other hand, rapidly increases the ratio of load capacities.

If the inboard bearing is offset from the center of the beam, the determination of the effect of shaft deflection is somewhat more complicated because the slope of the elastic curve becomes greater as the bearing is located toward the end of the beam. However, the load capacity of the offset bearing will fall somewhere between the capacities of an end bearing and a central bearing.

Total Load Capacity of a Central Bearing

The total load P of a central bearing may be determined from equations (16) by substituting $p = P/ld$ and $K = 0.133\,(3L/l - 1)$. The quantity $(3L/l - 1)$ is closely approximated by the simpler expression $3L/l$ for values of L greater than l by 3 or more. Thus, the following equations are obtained:

$$\frac{P}{(\mu N E^2)^{1/3}} \left(\frac{L}{d}\right)^{2/3} \left(\frac{l}{d}\right)^2 = \frac{1.46}{(l/d)^{1/3}} \qquad (\text{for } l/d \leqq 1.0) \tag{24a}$$

$$\frac{P}{(\mu N E^2)^{1/3}} \left(\frac{L}{d}\right)^{2/3} \left(\frac{l}{d}\right)^2 = \frac{1.46}{(l/d)} \qquad (\text{for } l/d \geqq 1.0) \tag{24b}$$

Equations (24) are plotted in figure 12 to show the total load capacity of a central bearing as the l/d ratio is varied by a change only in the bearing length l. As the bearing length approaches zero, the

load capacity approaches an infinite value, because the effect of the curvature of the deflected beam becomes small to permit the bearing to operate at an increasingly larger mean eccentricity. However, the load capacity of an extremely short bearing ultimately will be limited by the bearing surface roughness rather than by the deflection of the shaft.

Figure 12 also shows the lower load capacity of the bearing when the experimental hydrodynamic data of figure 4 are used rather than the analytical data where the coefficients in equations (24) are 1.10 instead of 1.46.

Equations (24) may be rearranged to show the variation of total load capacity with l/d where change in the bearing diameter d is the sole influence.

$$\frac{P}{(\mu N E^2)l/3}\left(\frac{L}{l}\right)^{2/3}\left(\frac{1}{l}\right)^2 = \frac{1.46}{(l/d)^3} \qquad (\text{for } l/d \leqq 1.0) \qquad (25a)$$

$$\frac{P}{(\mu N E^2)l/3}\left(\frac{L}{l}\right)^{2/3}\left(\frac{1}{l}\right)^2 = \frac{1.46}{(l/d)^{11/3}} \qquad (\text{for } l/d \geqq 1.0) \qquad (25b)$$

These equations are plotted in figure 13. The influence of l/d on load capacity where diameter is changed is much greater than where length is changed, as may be seen by comparing the curves of figure 13 and figure 12. Reducing l/d by increasing the diameter results in a rapid increase in beam stiffness so as to make the load capacity of the beam approach an infinite value as l/d approaches zero. However, both figures 12 and 13 show the same load capacity for $l/d = 1.0$.

Load Capacity of Run-in Bearings

With a careful run-in, bearings made of conformable materials may change shape under the loading of a hard journal on a flexible shaft. As shown in figure 3, the ends of the bearing may be deformed by pressure and rubbing such that the minimum end film thickness h_E is nearly uniform over the distance l' at the bearing ends. Two distinct regions of load-carrying film exist under these conditions: the deformed region and the undeformed region. After stabilization is reached in the running-in process, the thin film in the deformed region undoubtedly supports part of the bearing load, although the magnitude of this part is not known. Estimating its magnitude is complicated by the lack of information on the variation of the film thickness, which may be for either a fitted or an irregular wedge. In the undeformed region the film remains a wedge even in the neighborhood of closest approach.

A mathematical determination of the load-carrying capacity of a run-in bearing is difficult if both regions of supporting film are considered. However, if it is conservatively assumed that the end regions do not contribute to load support and that the film in the undeformed region supports the full load, then quantitative evaluation may be made. As deformation increases and l' increases, the effective length of the bearing is reduced; but because of the end deformation the bearing operates at a higher mean eccentricity and possibly at a higher load capacity.

For a central bearing the reduction in effective length may result in an increased load capacity as shown in figure 12, where load capacity increases as l/d becomes less. The load capacity may be even greater than shown in figure 12 because of the additional support of the deformed region. Running-in is normally manifest in a friction and temperature rise that may be temporary if end deformation permits the bearing to operate at a higher mean eccentricity and load capacity after the conditions stabilize. An end bearing, however, may show a decreased load capacity on running-in, as shown in figure 10(a), if the effective l/d ratio of the bearing is reduced to below 1. Presumably the friction and temperature rise in an end bearing would be greater than for a central bearing and may not stabilize because of the decreasing load capacity shown in figure 10(a). However, the degree to which the load support from the deformed end would alleviate the temperature rise is not known.

If in a given design it is known that a relatively high shaft flexibility under load would result in a deformed bearing, it would be advisable rather to scrape the surface to a bellmouth profile conforming to the bent shape of the journal. A circumferential wedge then would result for the full bearing length to give increased load capacity.

Surface Roughness

Certain of the curves, such as those of figures 11, 12, and 13, show that the load capacity of a bearing approaches an infinite value as the l/d of the bearing approaches zero. These curves indicate that, as a bearing becomes very short, the effect of shaft flexibility becomes of smaller importance and permits the bearing to operate at a high mean eccentricity. However, if metallic contact is the criterion of limiting the load capacity, roughness of the bearing surface becomes important.

Friction rise due to metallic contact begins where the highest asperities of the two surfaces first make contact. As shown in reference 4, an appreciable load-carrying film exists although failure may be imminent because of the friction rise. At the condition of first surface contact, the minimum film thickness h_{min} may be evaluated as the sum of the "predominant peak roughnesses" of the two surfaces. Tarasov (ref. 5)

has shown that "predominant peak roughness," which is a measure of true surface roughness, may be determined from profilometer measurements times a factor that depends on the method of finishing the surface. Reference 4 presents experimental data that show that for short bearings the load capacity may be predicted reasonably well from equation (7a) on the assumption that h_{min} is known from the surface roughnesses at initial metal contact.

Rearranging equation (7a) gives

$$\frac{p}{\mu N} = \frac{0.718}{\left(\frac{h_{min}}{d}\right)^2} (l/d)^2 \qquad (\text{for } l/d \leqq 1.0) \qquad (26)$$

Equation (26) gives unit load capacity as a function of l/d and the film thickness ratio h_{min}/d, in which h_{min} is assumed to be known from the surface roughness. The total load capacity may be determined by substituting $p = P/ld$.

$$\frac{P}{\mu N d^2} = \frac{0.718}{\left(\frac{h_{min}}{d}\right)^2} \left(\frac{l}{d}\right)^3 \qquad (\text{for } l/d \leqq 1.0) \qquad (27)$$

Equation (27), shown plotted in figure 14, is in a form that shows the effect on total load capacity of varying the l/d ratio by varying only the bearing length. The load capacity rises rapidly with increase in length and also rises rapidly as the surfaces more nearly approach the ideally smooth condition and permit operation on a thin film at impending contact of the surface asperities.

As discussed in the following section of this report, a number of experimenters have sought to determine the ideal l/d ratio of a heavily loaded bearing and have shown it to be in the region of the short bearing with l/d equal to or less than 1.0. By superimposing the total load capacity curve based on surface roughness on the curve based on shaft flexibility, an optimum l/d ratio is given by the intersection of the two curves. If in a given design situation of a central bearing all the variables are held constant except the bearing length, the load capacity P would vary with length l as shown by the intersecting curves of figure 15(a). The left curve would be from figure 14 for a given surface roughness, and the right curve would be for a given condition of shaft bending. The optimum length of the bearing for maximum load capacity is given by the intersection of the two curves.

Optimum l/d

Recognizing that shaft flexibility influences the load capacity of bearings, investigators such as Falz (ref. 6) and Deck (ref. 7) have experimentally determined l/d ratios giving maximum load capacity. Falz recommends values of l/d between 0.3 and 0.8, and Deck recommends values from 0.5 to 1.0. In the following paragraphs an illustrative example is presented and analyzed by using the equations of this report to support the findings of these investigators. The criteria used in the example include the influence of surface roughness as well as shaft deflection.

As shown in figure 15(a), this illustrative example is a symmetrically loaded, simple beam consisting of a 1.0-inch-diameter steel shaft with a beam length L of 3 inches between centers of the end bearings. For the shaft length chosen, space limitations allow a maximum l/d of approximately 1.5. A shaft speed of 6,000 rpm (100 rps) and a low viscosity of 1×10^{-6} reyn are assumed.

For the central bearing shown in figure 15(a), the dashed curve at the right gives unit load capacity for various l/d based on the criterion that h_E is zero because of beam deflection. The total load capacity P is first determined from the upper curve of figure 12 for various l/d and is then reduced to unit load capacity from $p = P/ld$.

The dashed curves at the left of figure 15(a) are based on the criterion that surface roughness limits the load capacity according to equation (26). Curves are shown for three minimum film thicknesses: $h_{min} = 0.000050$, 0.000025, and 0.0000125 inch. The value of 50 microinches represents a minimum film thickness for touching surface asperities when each surface has a measured roughness of 5 microinches root mean square. By the use of Tarasov's factor of approximately 5 for ground surfaces, the true roughness of each surface is approximately 25 microinches, giving a total of 50 microinches for h_{min} when asperities are at initial contact.

As shown in figure 15(a), the optimum l/d is at the intersection of the dashed curves based on the two separate criteria. It may be seen that the optimum l/d for a given design depends on the surface finish. For the roughest surfaces in figure 15(a), the optimum l/d is approximately 0.5, and for the smoothest surfaces approximately 0.25. These values agree in range with those obtained by Falz and Deck.

The curve of unit load capacity based on beam deflection in figure 15(a) is for the condition where the end minimum film thickness h_E is zero. However, since the surfaces are of some roughness, the first

metallic contact of the surfaces at the ends of the bearing is at the asperities of the surfaces, so that some end film thickness h_E other than zero exists. When the smoothest of the surfaces of the example is considered, h_E is 0.0000125 inch at first metallic contact. For this value of h_E, the unit load capacity may be determined from the more general expression of equation (9a).

$$\frac{h_E}{l} = 0.848 \sqrt{\frac{\mu N}{p}} - 0.94 \frac{k\delta}{l} \qquad (\text{for } l/d \leqq 1.0) \qquad (28)$$

For the central bearing of figure 15(a), $k = 0.8$ and δ is given by equation (21). By substituting the known variables of the illustrative example in equation (28) and assuming that $3r - 1 = 3r = 3L/l$ in equation (21), the following equation relates unit load capacity to bearing length:

$$12.5\times10^{-6} = 0.848\times10^{-2} \frac{l}{\sqrt{p}} - 0.0478\times10^{-6}\, p l^3 \qquad (29)$$

The curve from equation (29) is plotted as a solid line in figure 15(a) and shows the reduction in unit load capacity due to the assumption of a value of h_E greater than zero. The curve also shows that the optimum l/d is slightly reduced. It should be noted that the curve from equation (29) becomes tangent to the curve for surface roughness from equation (26). Solid-line curves are also shown for the other surface roughnesses and show the marked reduction in load capacity as the surfaces become rougher; also shown is the increase in optimum l/d.

Although the criterion that load capacity is limited by initial contact of surface asperities at the bearing edge is conservative, in an actual bearing this limit is not necessarily indicative of impending failure. With conformable materials, the surface roughness at the end of the bearing is relatively easily worn-in such that h_E may approach values close to zero. In this case, the unit load capacity curve would be somewhere between the solid curve and the higher dashed curve.

Figure 15(b) shows the curves from an analysis of the end bearings of the illustrative example. The curves shown are similar in form to those in figure 15(a) for the center bearing. However, the dashed curve for $h_E = 0$ is obtained from figure 10(a). The solid curves are determined from the general equation (28) with δ evaluated from equation (15) for an end bearing. Comparing the curves for the end bearings with those for the center bearing shows that the load capacities are smaller and that the optimum l/d indicates use of a shorter bearing. This is realistic since the slope of the elastic curve is greater for the end bearings than for the center bearing.

EXPERIMENTAL DATA

Battelle Memorial Tests

In experiments to determine the mechanism of hydrodynamic failure in journal bearings, Dayton, Allen, Davis, and Austin of Battelle Memorial Institute (ref. 8) report unit load capacities of heavily loaded bearings in excess of 10,000 psi before failure by seizure. Tests of bearings of various materials, principally copper, babbit, and copper-lead, were made with the simply supported beam shown in figure 16. The test bearing was a central bearing on a short shaft supported at the ends in roller bearings. Load was applied through a ball at the top of the central bearing to insure alinement of loading. The test bearings were 1.25 inch in diameter and 1.0 inch long with a diametral clearance of 0.002 inch. SAE 10 oil preheated to 200° F was pressure fed at 40 pounds per square inch gage. The bearings were also preheated to 200° F. Shaft speed was 6,000 rpm.

In the tests the load was applied slowly in increments of 500 psi. With each load increase, the temperature rose slightly. However, each succeeding increase was made after the temperature reached equilibrium in about 3 minutes. By using this careful low-rate loading procedure, high load capacities were achieved with an average temperature rise of approximately 20° F. The following values of unit load were attained at seizure for various bearing materials:

Copper	Above 10,000 psi
Copper-lead	7,500 to 8,000 psi
Babbitt	Above 10,000 psi

As the Battelle experimenters point out, all the bearing materials, even those usually regarded as poor, exhibited a high load capacity when tested under careful conditions.

Calculations of the load capacity of the test bearings from the equations of this report show a high load capacity, although the magnitude is somewhat less than those obtained in the tests. With an l/d of 0.8 for the test bearings, the upper curve of figure 12 gives the following equation for determining the load capacity at the condition for impending metallic contact of the central bearing:

$$\frac{P}{(\mu N E^2)^{1/3}} \left(\frac{L}{d}\right)^{2/3} \left(\frac{l}{d}\right)^2 = 1.56 \qquad (30)$$

For the Battelle tests the following quantities are assumed: $d = 1.25$ inch, $L/d = 2.0$, $N = 100$ rps, and $E = 30 \times 10^6$ psi for steel. Although the exact value for viscosity is not known, the chart value for SAE 10 oil at 220° F is approximately 5 centipoises or 0.7×10^{-6} reyn. Substituting these quantities in equation (30) gives the following values of load capacity:

$P = 6{,}100$ lb (total load)
$p = 4{,}900$ psi (unit load)

By assuming that the lower curve of figure 12 should be used for a conservative estimate of load capacity, then $P = 4{,}600$ pounds and $p = 3{,}700$ psi.

The calculated load capacities are between a half and a third of the capacities obtained in the tests. However, the slow rate of loading in the tests indicates that run-in was an important factor. According to the curves of figure 12, to achieve a load capacity of two to three times the calculated values just given, the bearings might have been deformed 90 percent of the length or more in the running-in procedure.

In subsequent tests at Battelle Memorial Institute by Dayton, Allen, Fawcett, and Miller (ref. 9), seizure tests were made while measuring minimum film thickness by the dielectric breakdown method. The same testing machine was used for tests at speeds of 5,800, 3,600, and 2,200 rpm. Load capacities at seizure were somewhat lower than in the previous tests, but the materials tested were different. The following table shows a comparison of the calculated load capacities from the upper curve of figure 12 and the experimental ones for the three speeds. Since in all tests the bearings and the SAE 10 oil were preheated to 200° F, the value of $\mu = 0.7 \times 10^{-6}$ reyn is used for the calculated load capacities.

Material	Unit load capacity, p, psi					
	At 5,800 rpm		At 3,600 rpm		At 2,200 rpm	
	Test	Calc.	Test	Calc.	Test	Calc.
25 Aluminum	5,400	4,800	-----	4,100	-----	3,500
72-25-3 Alloy	6,800	4,800	-----	4,100	-----	3,500
Bronze	7,400	4,800	4,400	4,100	2,600	3,500
Tin-base babbit	5,000	4,800	4,000	4,100	3,300	3,500

The table indicates that the order of magnitude of bearing capacity is reasonably well predicted from the equations of this report and that failures of the bearings in the tests may have been caused principally by journal deformation.

Data by Falz

Falz's report (ref. 6) concerns the design of short journal bearings, and from experimental findings he recommends that the l/d ratio should be between 0.3 and 0.8 for best load-carrying capacity to take into account the effect of beam deflection. In his report, the curves given herein as figure 17 are presented to show the effect of l/d on load capacity. Experimental points are shown, although details of the experiment are not given. As shown in figure 17, the unit load capacity p rises rapidly as the bearing is made shorter to a lower limit of l/d approximately equal to 0.2. As the bearing l/d approaches the very small values near zero, the load capacity then decreases to zero at a rapid rate.

The Falz curve of unit load capacity may be compared with the analytically determined curves of the illustrative example (fig. 15). The analytical curves are similar in form and show that the optimum value of l/d is in the range of the short bearing having low l/d values. The analytical curves show the steep gradients on either side of the optimum l/d as shown in the experimental curve. However, the gradients are less steep as h_E becomes greater, because of surface roughness at the bearing end. It is possible that in the Falz experiments surface roughness at the bearing ends was a relatively minor factor, because wearing-in at the bearing ends may have caused a reduction of h_E to near zero. If so, the gradients of the experimental curve would be those approaching the dashed lines of figure 15. The experimental and analytical curves are not compared for quantitative values, since the conditions of speed, viscosity, and beam configuration of the experiments are not known.

Figure 17 gives the Falz experimental curve of total load capacity P, which depends on both the unit load capacity p and l/d. As shown, the optimum l/d based on total load is approximately 0.5 and is greater than the value based on unit load. In any given design, the recommended l/d would be that for total load rather than unit load.

For comparison with the Falz experimental curve for total load capacity, the analytically determined curves of figure 18(b) give the illustrative example. Comparing the curve for the center bearing with Falz's experimental curve shows that the shapes are in general similar and that by coincidence the optimum l/d ratios are nearly the same, both being approximately 0.5. However, the shape of the analytical curve for the end bearings in figure 18(b) is somewhat different from the center bearing. The optimum l/d for the end bearing is 1.0 for total load capacity, although the optimum l/d for unit load capacity is less than 0.2 as shown in figure 15(b). The curves in figure 18(b) are determined from the curves of unit load capacity in figure 15 for $h_E = 0.0000125$ inch.

Figure 18(b) gives a comparison of the order of magnitude of the total load capacities of the center and end bearings of the illustrative example. The capacity of the end bearing is much less than the center bearing, although in a simple beam the end bearings are required to have half the capacity of the center bearing. The difference in the capacities of end and center bearings would be less as the beam configuration is made stiffer by an increase in bearing diameter or by a shortening of beam length.

Data by Deck

Figure 18(a) gives experimental data presented by Deck (ref. 7) of total load capacity against l/d for aluminum bearings. A comparison of these data with the analytical curves of figure 18(b) shows that for the central bearing the form of the curves is similar in some respects. The data of the experimental and analytical curves are not directly comparable, since the conditions of the experiments are not known; although, by coincidence, values of capacity are of the same order of magnitude for the central bearing. On the basis of the experimental data, Deck recommends that bearings should have l/d from 0.5 to 1.0 to minimize end pressure due to beam deflection. The analytical curves of figure 18(b) indicate that Deck's lower l/d value would apply to central bearings, and the upper value to end bearings.

DISCUSSION

Although bearing designers know that shaft deflection and surface irregularities reduce bearing load capacity to less than the infinite value predicted by hydrodynamic theory, these limiting variables have been considered too complex for mathematical treatment. In reference 4, the effect of bearing surface roughness on load capacity is treated analytically. The purpose of the present report is to show that the shaft deflection problem also may be solved analytically to yield design data of a useful order of magnitude.

Although other factors such as local high spots, out-of-roundness, out-of-straightness, grit, lubricant corrosion, and corrosive atmospheres also limit bearing capacity and life, shaft deflection and surface roughness appear to be of first-order importance in limiting the capacity of heavily loaded bearings. The analysis presented herein is an attempt to seek out the limits of thick film lubrication as the region of boundary lubrication is approached. High load capacities may be achieved by promoting conditions that permit an extremely small film thickness to exist free of asperities causing metallic contact. A careful running-in or wearing-in may in many cases increase load capacity because the burnishing action permits a smaller film to exist without a friction rise by metallic contact.

It should be noted that the bearing clearance is not included in the equations of this report. Rather, the load-carrying capacity of the film is based on minimum film thickness h_{min}, as given by equations (7) and (26). According to assumptions in reference 4, load capacity of the film is nearly independent of clearance in heavily loaded bearings where the eccentricity ratio exceeds 0.6. This is because $f(n)$ in equation (4) varies only slightly at the high eccentricity ratios.

Based on the short-bearing approximation (ref. 1), the average value of $f(n)$ is taken as 0.718. However, the experimental data in figure 4 show higher eccentricity ratios or smaller film thicknesses for the same loading. Thus, a value of $f(n) = 0.30$ has been used to represent the experimental data for hydrodynamic capacity. As shown in figures 9 to 13, bearing load capacities are given for $f(n)$ of 0.718 and 0.30. A designer may wish to use a value of $f(n)$ that from these or other experimental hydrodynamic data seems better to apply. In this sense a designer may choose a conservative value of $f(n)$ as a factor of safety. Also, a designer may evaluate load capacity P on the basis of $f(n)$ of 0.718 or 0.30 and divide this load by a suitable factor of safety greater than 1.0.

The Battelle Memorial tests indicate that by a careful, slow run-in of a central bearing high load capacities can be attained. The capacity that can be attained depends on the bearing material and the degree to which the material can be made to conform to the shape of the bent journal. It is interesting that the Battelle experimenters report a temperature rise near seizure of only 20° to 50° F higher than the 200° F to which the oil and bearings were preheated. This appears to indicate that, after the transient phase when the bearing material deforms, the load continues to be carried hydrodynamically. The assumption that run-in reduces the effective length of the bearing is conservative, since no hydrodynamic load capacity is attributed to the deformed lengths l' at the bearing ends. This assumption may be realistic if the deformed surfaces are considered to be fitted ones where no circumferential wedge action can take place to carry the load hydrodynamically. If the bearing ends were deformed completely around the circumference in a bellmouth form, wedge action is possible so that hydrodynamic support would be realized at the deformed ends and result in a higher load capacity. By scraping the bearing to a bellmouth profile having the shape of the bent journal, the load capacity could be increased to very high magnitudes. Scraping of bearings to bellmouth or conical ends has been utilized for many years as a practical means of increasing the load capacity of bearings with deflecting shafts.

The curves of figure 9 are the most general ones for predicting the unit load capacity of a bearing where shaft flexibility is a variable. The curves include all possible cases of beam loading so long as the

appropriate value of K is used. With experience, a suitable value of K may be determined from calculations and judgment even for complex beam loadings. For the elementary cases of beam loading, however, the load capacities of central and end bearings are most directly determined from the curves of figures 10 to 13.

CONCLUSIONS

The following conclusions may be drawn from the results of this investigation of the influence of shaft deflection and surface roughness on the load-carrying capacity of full journal bearings:

1. The limiting load capacity of a journal bearing is predictable to a reasonable order of magnitude by including shaft deflection or surface roughness as the limiting factor.

2. In the absence of self-alining characteristics, the elastic curvature of the shaft is a major limiting factor, and its effect increases with bearing length. The analytical curves of this report substantiate the experimental findings of Falz and Deck that the optimum length-diameter ratio of a bearing is in the region from 0.3 to 1.0 for maximum load capacity. Each design case, depending on beam configuration and surface finish, is unique. The optimum length-diameter ratio for a given configuration is predictable to a reasonable order of magnitude.

3. Preforming a central bearing to conform to the shape of a journal deflected by a given load tends to counteract the effect of elastic deflection, so that surface finish becomes the limiting factor.

4. For heavy loading, this report indicates a distinction between end bearings and central bearings such that end bearings benefit by self-alining or equivalent elastic mountings, but that central bearings even if self-alined will benefit by performing to a bellmouth shape. The curves presented facilitate estimating the magnitude of the benefit.

Cornell University,
Ithaca, N. Y., August 15, 1957.

APPENDIX A

DETERMINATION OF MINIMUM END CLEARANCE

The geometry of figure 2 indicates that the minimum film thickness or minimum end clearance h_E may be expressed as follows:

$$h_E = c_r - \sqrt{e^2 + k^2\delta^2 + 2ek\delta \cos \varphi}$$

This equation may be generalized by letting A equal the ratio of $k\delta$ to the eccentricity e; that is, $A = k\delta/e$; thus, the equation becomes

$$h_E = c_r - e\sqrt{1 + A^2 + 2A \cos \varphi} \tag{A1}$$

For most bearing operating situations, the term A is considerably less than 1. Thus, the quantity $e\sqrt{1 + A^2 + 2A \cos \varphi}$ may be closely approximated by the expression $e(1 + A \cos \varphi)$. The error resulting from this approximation is evaluated in the following manner. By using this latter expression in equation (A1), the approximate equation for the minimum film thickness at the end of a bearing is found to be

$$h_E = c_r - e(1 + A \cos \varphi) \tag{A2}$$

The range over which equation (A2) yields the best approximation may be determined by computing the ratio of the error in h_E to the radial clearance c_r:

$$\Delta = \frac{(h_E)_{approx.} - (h_E)_{exact}}{c_r}$$

$$\Delta = n(1 + A \cos \varphi) - n\sqrt{1 + A^2 + 2A \cos \varphi} \tag{A3}$$

where Δ is the ratio of error in h_E to radial clearance c_r.

The attitude angle φ may be calculated as a function of eccentricity ratio n (ref. 1), in the following manner:

$$\varphi = \tan^{-1}\left[\frac{\pi}{4}\frac{(1 - n^2)^{1/2}}{n}\right] \tag{A4}$$

From equations (A3) and (A4), the variation of Δ as a function of φ and A may be determined as shown in the following table:

VALUES OF ERROR RATIO Δ			
φ, deg	A = 1.0	A = 0.1	A = 0.01
0	0.000	0.000	0.000
10	.005	.000	.000
20	.020	.000	.000
30	.055	.001	.000
40	.075	.002	.000
50	.090	.002	.000
60	.094	.002	.000
70	.083	.001	.000
80	.050	.001	.000
90	.000	.000	.000

This table clearly indicates that for values of A of 0.1 or less the error ratio is quite negligible. As A approaches 1, the error ratio begins to be appreciable. In any practical bearing design, the value of A would seldom if ever approach 1. For most designs A will be less than 0.1.

Experiment (ref. 1) shows that, as the eccentricity ratio approaches unity, the attitude angle approaches 20° rather than 0° according to theory. This indicates that the term $e\sqrt{1 + A^2 + 2A \cos \varphi}$ might better be approximated by $e(1 + A \cos 20^\circ)$, especially in the vicinity where n approaches 1; that is,

$$e\sqrt{1 + A^2 + 2A \cos \varphi} = e(1 + A \cos 20^\circ) \tag{A5}$$

With this latter approximation, equation (A3) becomes

$$\Delta' = n(1 + A \cos 20^\circ) - n\sqrt{1 + A^2 + 2A \cos \varphi} \tag{A6}$$

where Δ' is the error incurred by approximating $\sqrt{1 + A^2 + 2A \cos \varphi}$ with $(1 + A \cos 20^\circ)$.

From equations (A4) and (A6) the following table of error ratios is determined:

VALUES OF ERROR RATIO Δ'			
φ, deg	A = 1.0	A = 0.1	A = 0.01
0	0.060	0.006	0.001
10	.050	.004	.000
20	.025	.000	.000
30	.005	.005	.000
40	.042	.008	.001
50	.067	.014	.001
60	.088	.016	.002
70	.082	.015	.001
80	.058	.009	.001
90	0	0	.000

This table shows that in general the errors resulting from the use of $(1 + A \cos 20^{\circ})$ are larger than for $(1 + A \cos \varphi)$. However, since $(1 + A \cos 20^{\circ})$ is based on experimental findings for the region of $\varphi < 20^{\circ}$ and since the errors in the region $20^{\circ} < \varphi < 0^{\circ}$ are relatively small, the use of this approximation seems justified.

Thus, substituting the approximation indicated by equation (A5) into equation (A1) gives:

$$h_E = (c_r - e) - 0.94k\delta$$

$$h_E = h_{min} - 0.94k\delta \qquad \text{(A7)}$$

APPENDIX B

DEFLECTION OF JOURNAL AT END BEARING OF CANTILEVER BEAM

The equation for the slope of the deflection curve at the end of a cantilever beam as shown in figure 8 is known to be

$$\beta = \frac{PL^2}{2EI} \tag{B1}$$

For the end bearing of a cantilever beam P equals pld, and for a circular shaft I equals $\frac{\pi d^4}{64}$. Substituting the preceding expressions into equation (B1) gives

$$\beta = \frac{32p}{\pi E}\left(\frac{l}{d}\right)^3 r^2 \tag{B2}$$

The deflection δ within the half-length of the bearing may be obtained by multiplying β of equation (B2) by one-half the length of the bearing. Therefore,

$$\delta = \frac{4pl}{\pi E}\left(\frac{l}{d}\right)^3 4r^2$$

$$\delta = \left[\frac{4}{\pi}\frac{pl}{E}\left(\frac{l}{d}\right)^3\right]K$$

where

$$K = 4r^2 = 4(L/l)^2$$

APPENDIX C

TOTAL LOAD CAPACITY OF END BEARING OF CANTILEVER BEAM

The equations for the capacity of the end bearing of a cantilever shaft are determined from equations (16) by substituting $K = 4r^2 = 4(L/l)^2$ from appendix B.

$$\frac{P}{(\mu NE^2)^{1/3}}\left(\frac{L}{d}\right)^{4/3}\left(\frac{l}{d}\right)^2 = 0.315\left(\frac{l}{d}\right)^{1/3} \qquad \left(\text{for } \frac{l}{d} \leqq 1.0\right) \quad (C1)$$

$$\frac{P}{(\rho NE^2)^{1/3}}\left(\frac{L}{d}\right)^{4/3}\left(\frac{l}{d}\right)^2 = 0.315/(l/d)^2 \qquad \left(\text{for } \frac{l}{d} \geqq 1.0\right) \quad (C2)$$

Equations (C1) and (C2) provide a convenient means of determining the variation of the total load capacity with the <u>length</u> of the bearing as shown by figure 10(a). These equations may be rewritten in the following manner to determine the variation of the total load capacity with the <u>diameter</u> of the bearing as shown in figure 11(a).

$$\frac{P}{(\mu NE^2)^{1/3}}\left(\frac{L}{l}\right)^{4/3}\left(\frac{l}{l}\right)^2 = \frac{0.315}{(l/d)^3} \qquad (\text{for } l/d \leqq 1.0) \quad (C3)$$

$$\frac{P}{(\mu NE^2)^{1/3}}\left(\frac{L}{l}\right)^{4/3}\left(\frac{l}{l}\right)^2 = \frac{0.315}{(l/d)^{11/3}} \qquad (\text{for } l/d \geqq 1.0) \quad (C4)$$

APPENDIX D

CALCULATION OF δ FOR CENTRAL BEARING

The equation of the elastic curve of a simply supported beam with a concentrated load at its center as shown by figure 1(b) is

$$y_x = \frac{Px}{48EI}\left(3L^2 - 4x^2\right) \qquad \left(\text{for } 0 \leqq x \leqq \frac{L}{2}\right) \qquad \text{(D1)}$$

The maximum deflection occurs at the center of the beam and is determined by letting $x = \frac{L}{2}$ in equation (D1); thus,

$$y_{max} = \frac{PL^3}{48EI} \qquad \text{(D2)}$$

The deflection from the center of the beam to some station x is calculated by subtracting equation (D1) from equation (D2). Therefore,

$$y_{L/2} - y_x = \frac{P}{48EI}\left(L^3 - 3L^2x + 4x^3\right) \qquad \text{(D3)}$$

The deflection δ from the center of the bearing to the end of the bearing is readily found by letting $x = \frac{L - l}{2}$ in equation (D3):

$$\delta = \frac{Pl^2}{96EI}\left(3L - l\right) \qquad \text{(D4)}$$

The latter equation may be expressed more directly in terms of the bearing geometry by letting $r = L/l$, the ratio of the shaft span to the length of bearing. Since $I = \frac{\pi D^4}{64}$ and $P = pld$, equation (D4) becomes

$$\delta = \frac{2}{3}\frac{pl}{\pi E}\left(\frac{l}{d}\right)^3 (3r - 1)$$

$$\delta = \left[\frac{4}{\pi}\frac{pl}{E}\left(\frac{l}{d}\right)^3\right] 0.167\,(3r - 1)$$

REFERENCES

1. DuBois, George B., and Ocvirk, Fred W.: Analytical Derivation and Experimental Evaluation of the Short-Bearing Approximation for Full Journal Bearings. NACA Rep. 1157, 1953. (Supersedes NACA TN's 2808 and 2809.)

2. DuBois, G. B., Ocvirk, F. W., and Wehe, R. L.: Experimental Investigation of Eccentricity Ratio, Friction, and Oil Flow of Long and Short Journal Bearings with Load-Number Charts. NACA TN 3491, 1955.

3. DuBois, G. B., Ocvirk, F. W., and Wehe, R. L.: Experimental Investigation of Misalining Couples and Eccentricity at Ends of Misalined Plain Bearings. NACA TN 3352, 1955.

4. Ocvirk, F. W., and Dubois, G. B.: Relation of Journal Bearing Performance to Minimum Oil-Film Thickness. NACA TN 4223, 1958.

5. Tarasov, L. P.: Relation of Surface-Roughness Readings to Actual Surface Profile. Trans. ASME, vol. 67, no. 3, Apr. 1945, pp. 189-196.

6. Falz, E.: Narrow Sleeve Bearings. Product Eng., vol. 17, no. 8, Aug. 1946, pp. 113-115.

7. Deck, A.: Aluminum-Alloy Bearings. Light Metals, vol. 8, no. 95, Dec. 1945, pp. 579-591. (See also Product Eng., vol. 17, no. 2, Feb. 1946, pp. 128-130.)

8. Dayton, R. W., Allen, C. M., Davis, K. A., and Austin, A. E.: A Fundamental Study of Bearing Behavior. Battelle Memorial Inst., Mar. 31, 1950. (Contract N5-ori-111.)

9. Dayton, R. W., Allen, C. M., Fawcett, S. L., and Miller, N. E.: A Fundamental Study of Bearing Behavior. Battelle Memorial Inst., Dec. 31, 1952. (Contract N5-ori-111.)

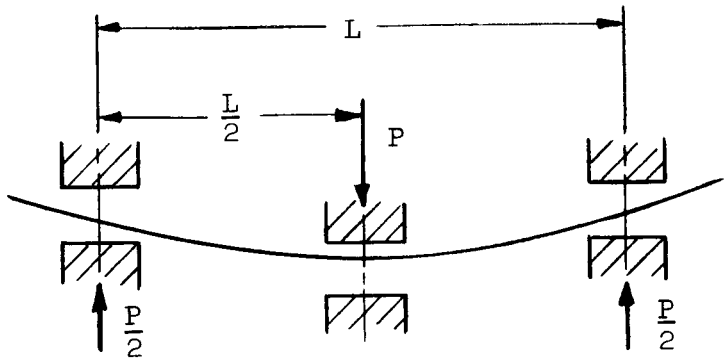

(a) Centrally loaded shaft.

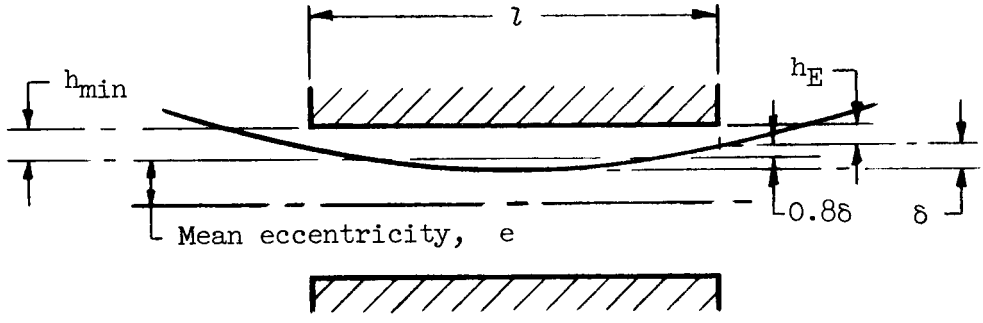

(b) Center bearing.

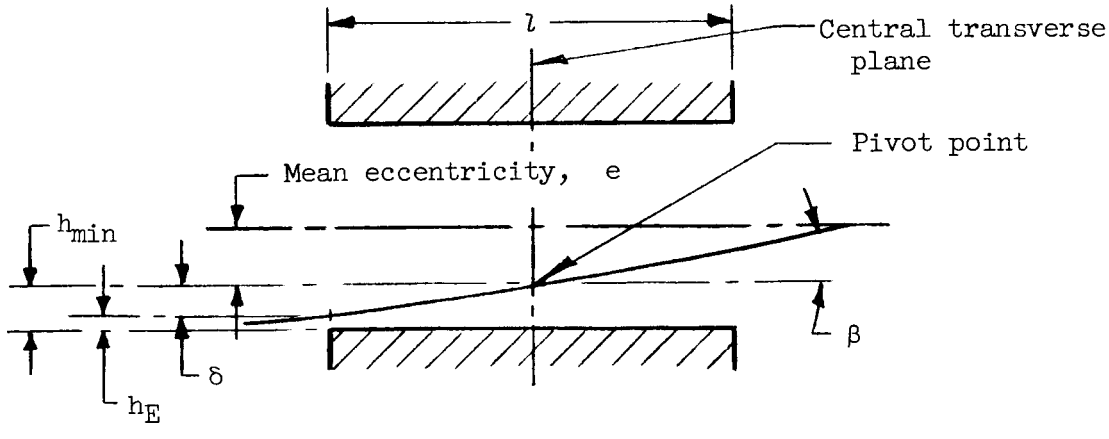

(c) End bearing.

Figure 1.- Shaft deflection in relation to journal bearings.

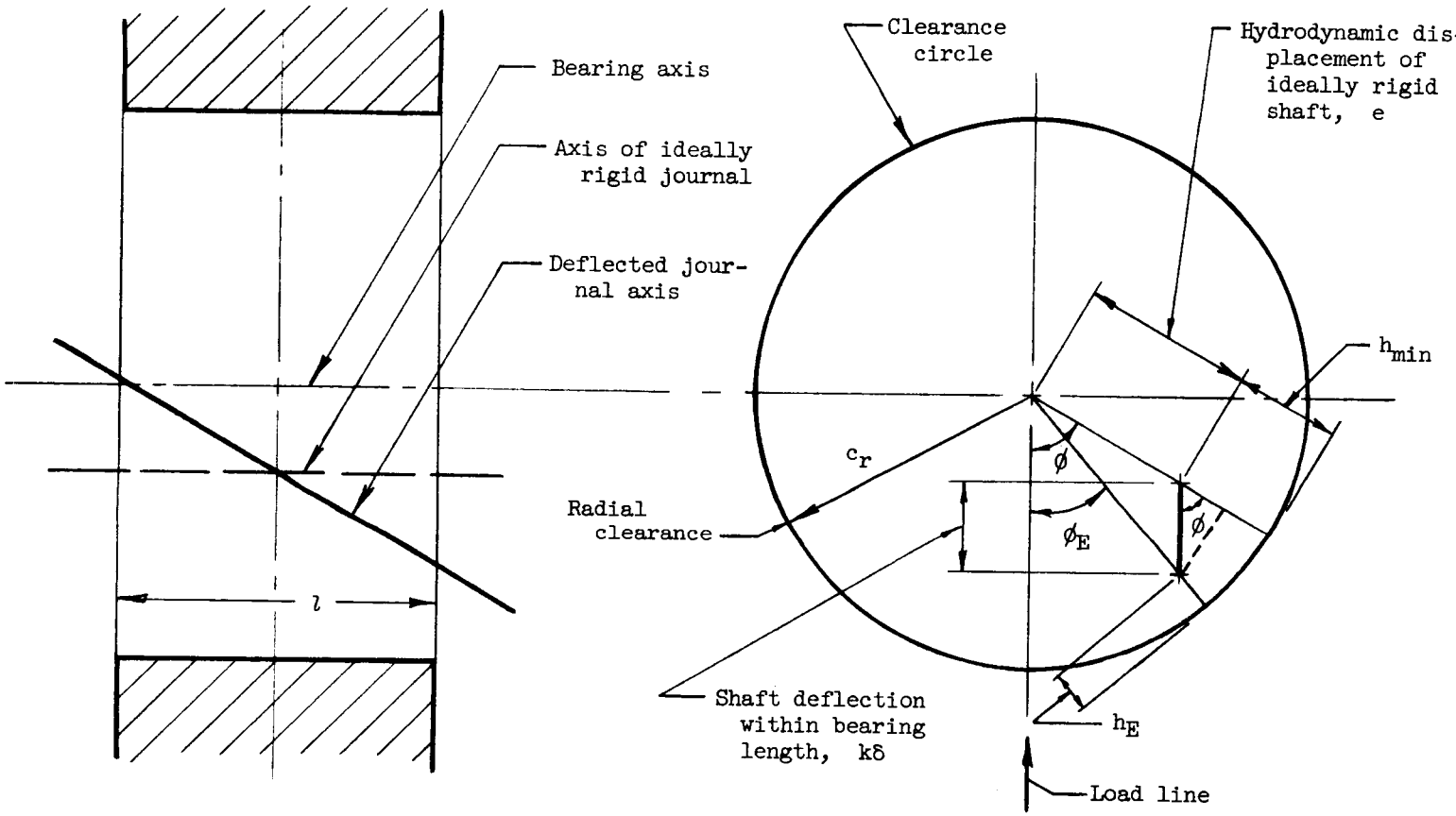

Figure 2.- Attitude of elastically deflected journal in a bearing. Clearance circle diagram shows geometric relation of minimum end film thickness h_E to mean minimum film thickness h_{min} and shaft deflection $k\delta$.

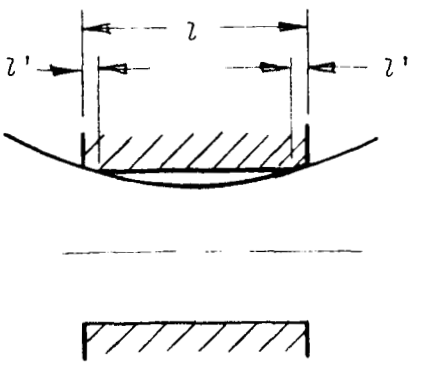

(a) Central bearing.

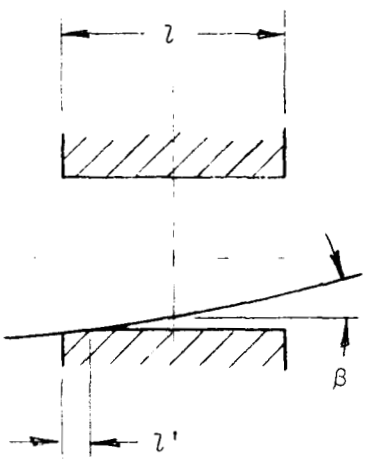

(b) End bearing.

Figure 3.- Effect of run-in on bearings of conformable material. Bearing ends are deformed to shape of bent shaft by careful run-in.

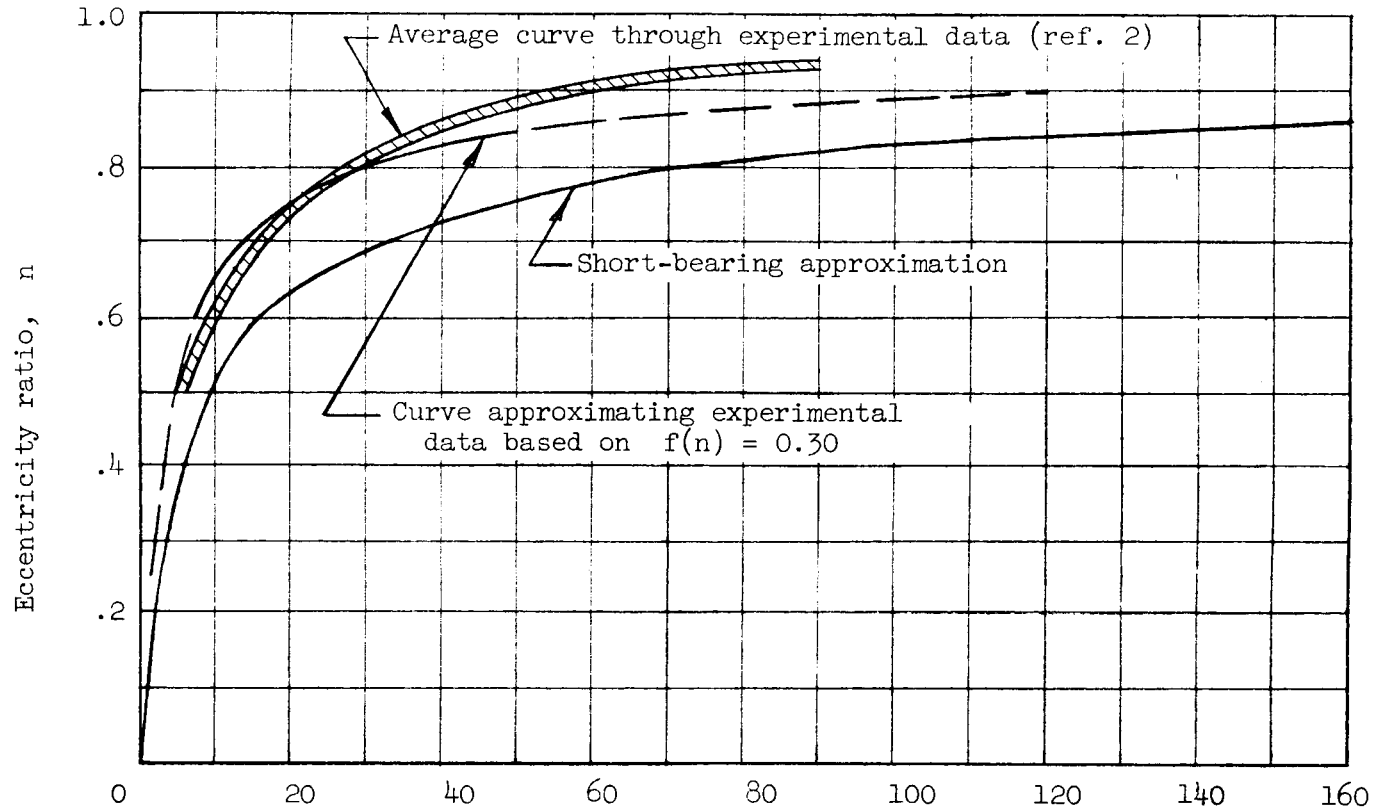

$$\text{Load number} \begin{cases} \dfrac{l}{C_n} = \dfrac{p}{\mu N}\left(\dfrac{C_d}{d}\right)^2\left(\dfrac{d}{l}\right)^2 & \text{for } \dfrac{l}{d} \leqq 1.0 \\ \dfrac{l}{S} = \dfrac{p}{\mu N}\left(\dfrac{C_d}{d}\right)^2 & \text{for } \dfrac{l}{d} \geqq 1.0 \end{cases}$$

Figure 4.- Eccentricity ratio against load number.

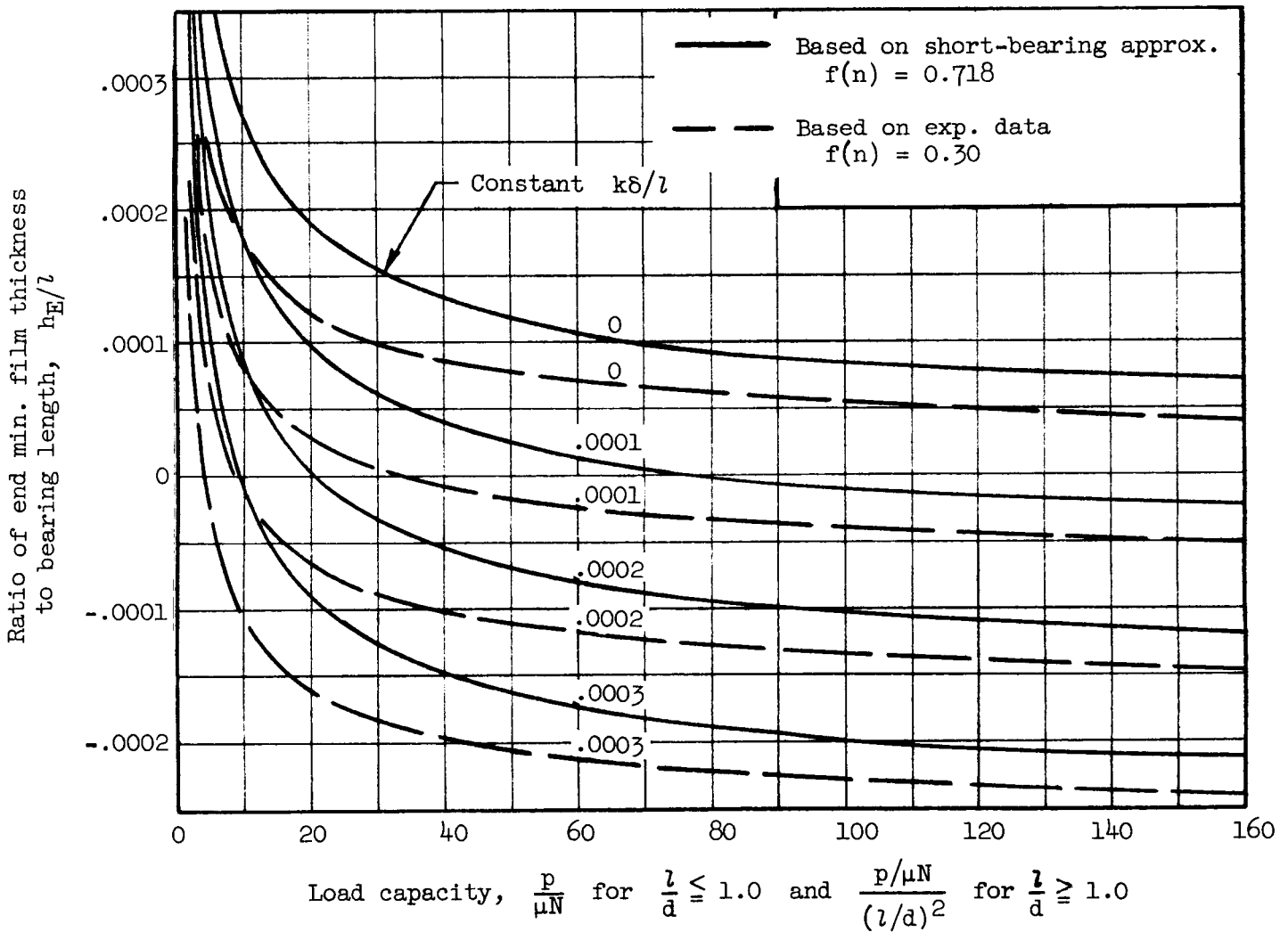

Figure 5.- End minimum film thickness as function of load capacity and shaft deflection for eccentricity ratios greater than 0.6.

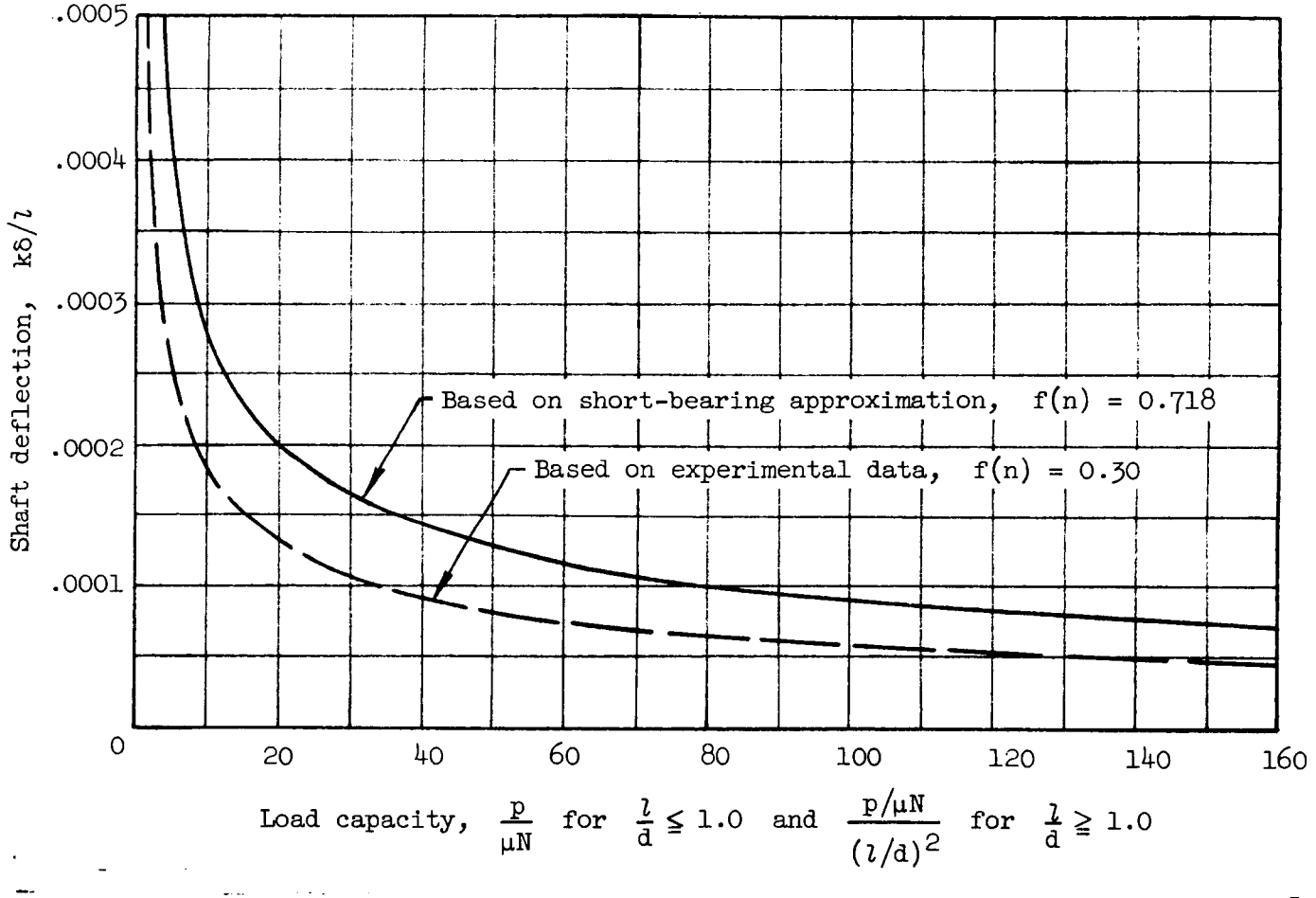

Figure 6.- Load capacity as function of shaft deflection at impending contact of surfaces ($h_E = 0$) for eccentricity ratios greater than 0.6.

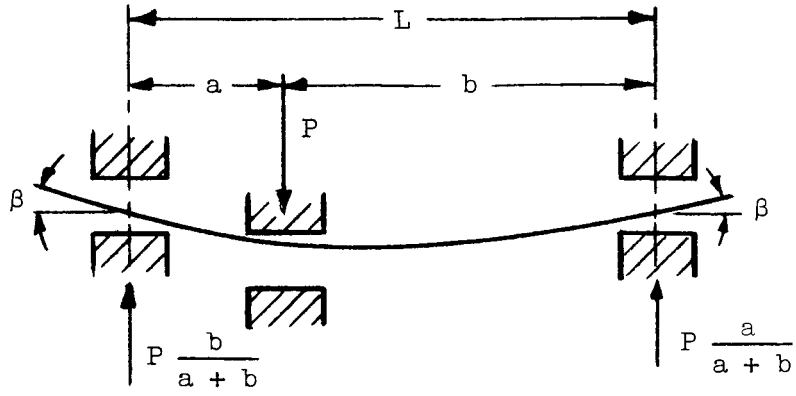

Figure 7.- Unsymmetrical loading condition of simply supported shaft showing attitude of deflected shaft to end bearings.

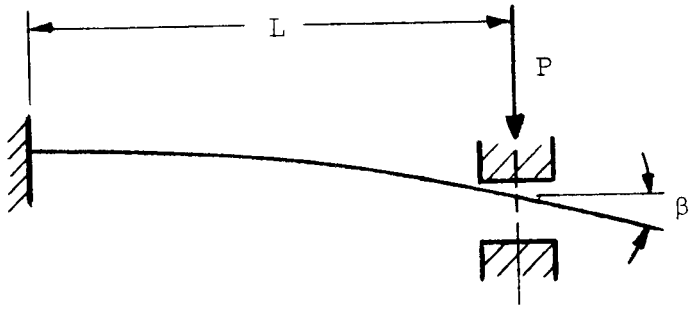

Figure 8.- Cantilever shaft loading condition.

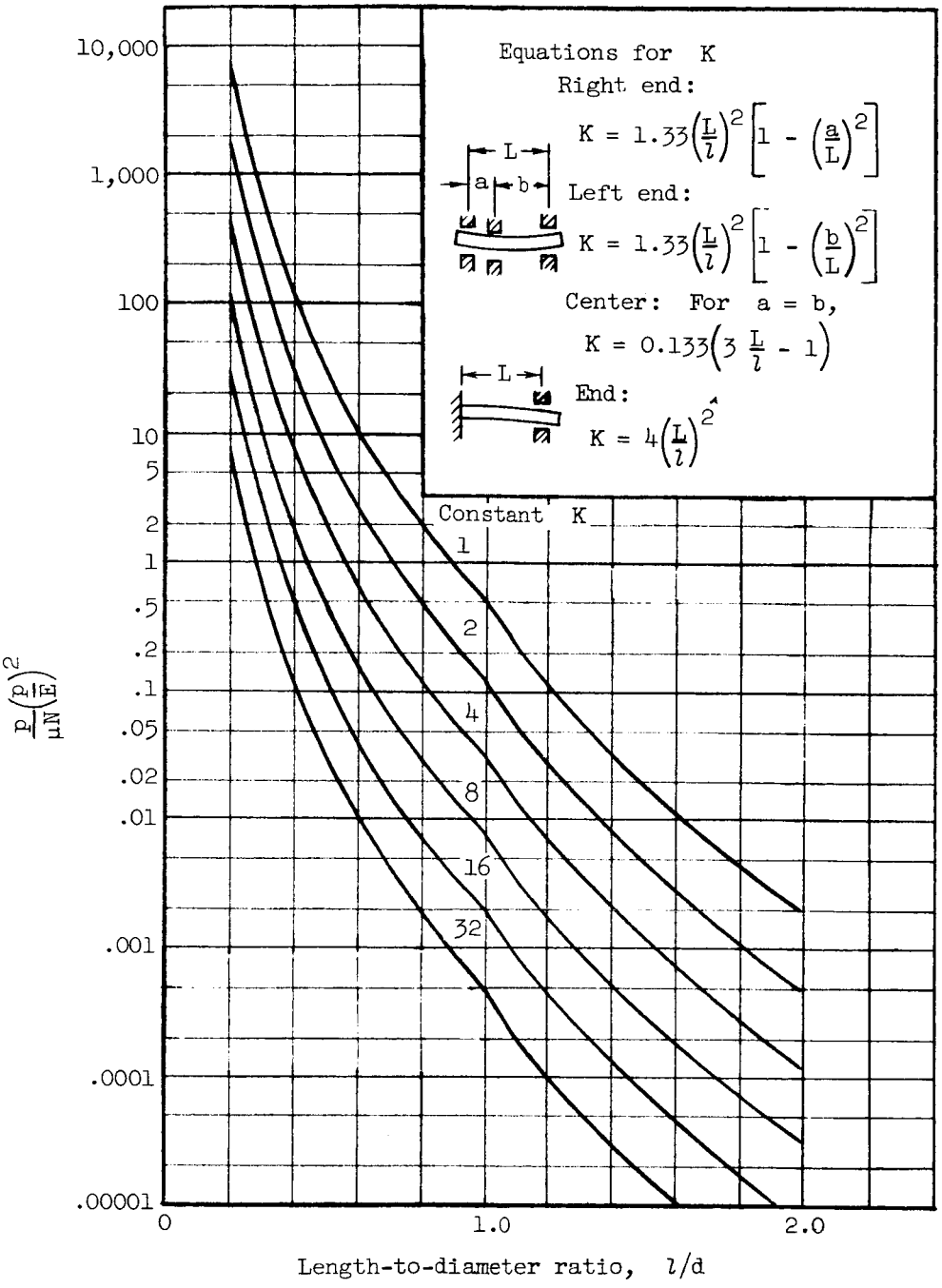

(a) Based on short-bearing approximation, $f(n) = 0.718$.

Figure 9.- Unit load capacity of a bearing against l/d at impending contact of surfaces ($h_E = 0$) due to shaft deflection.

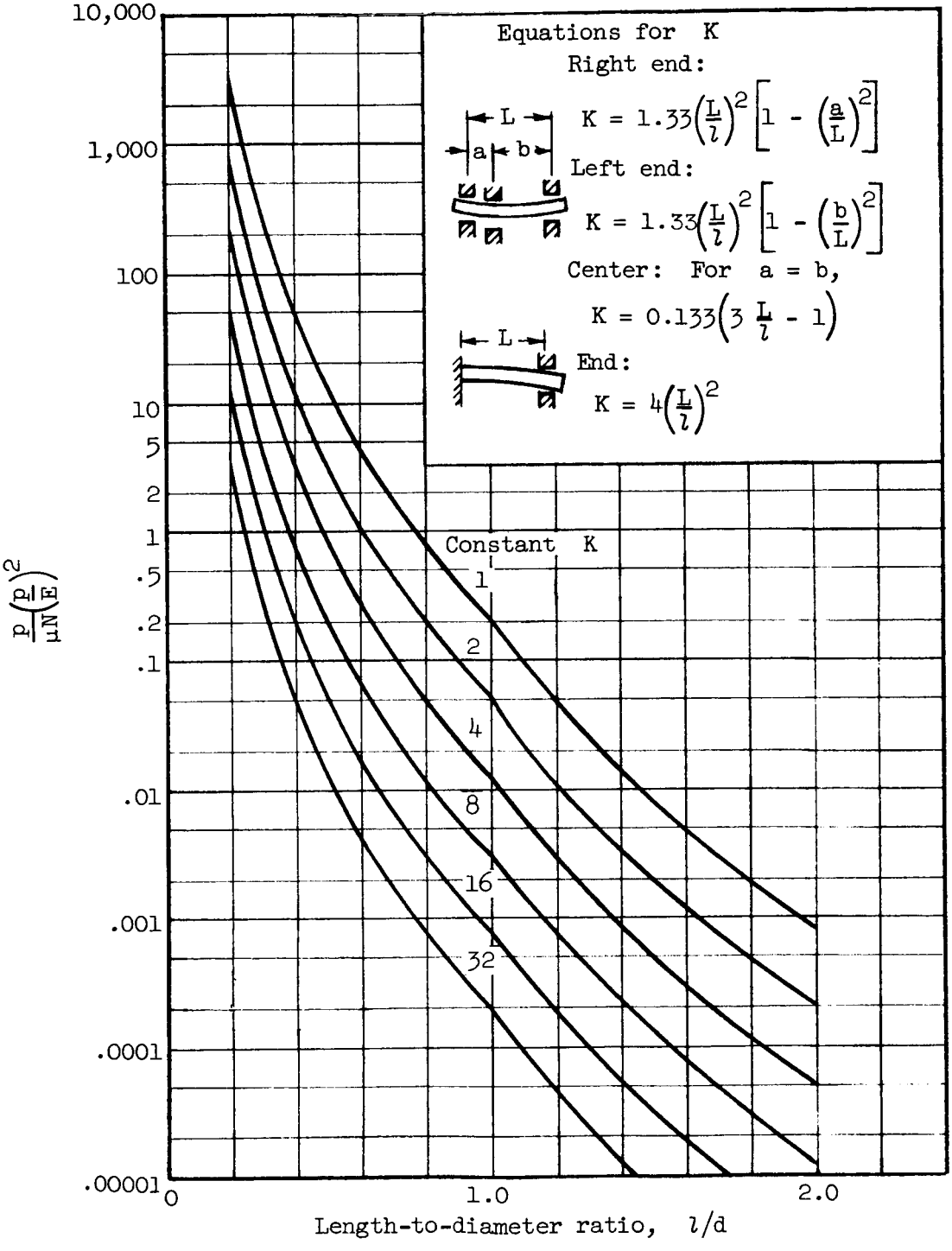

(b) Based on experimental hydrodynamic data, f(n) = 0.30.

Figure 9.- Concluded.

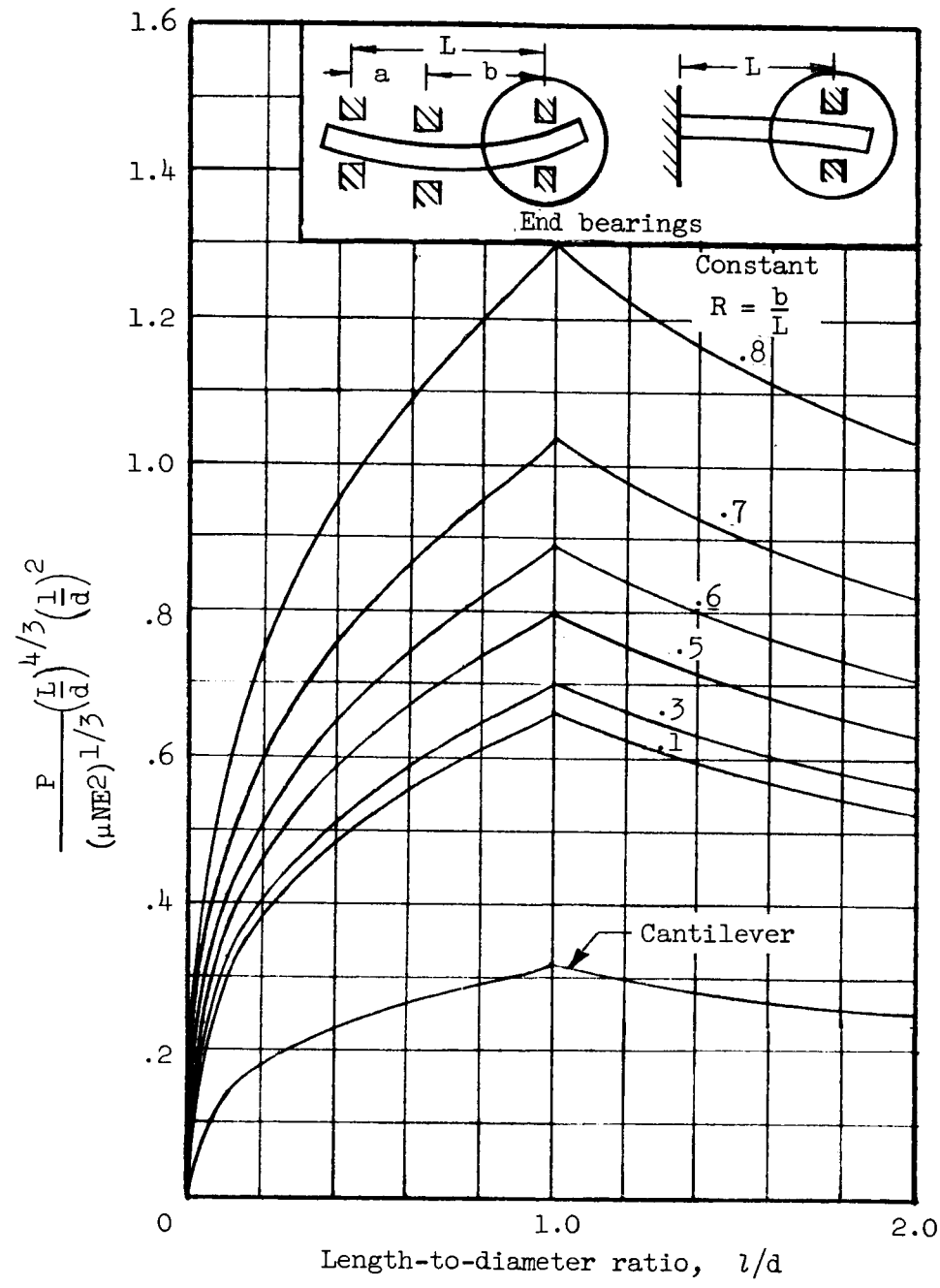

(a) Based on short-bearing approximation, f(n) = 0.718.

Figure 10.- Total load capacity of end bearings against bearing length at impending contact of surfaces due to shaft deflection.

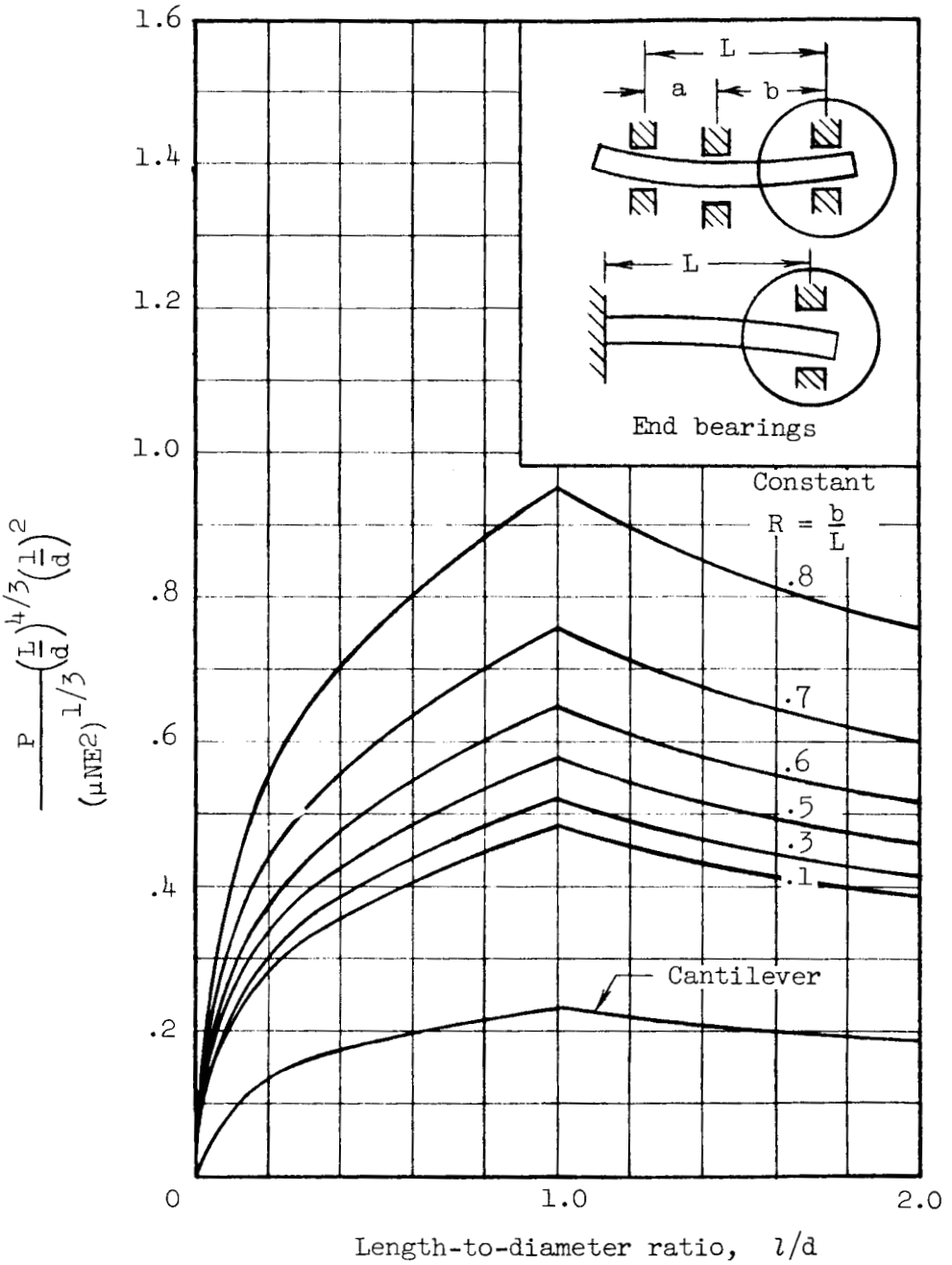

(b) Based on experimental data, f(n) = 0.30.

Figure 10.- Concluded.

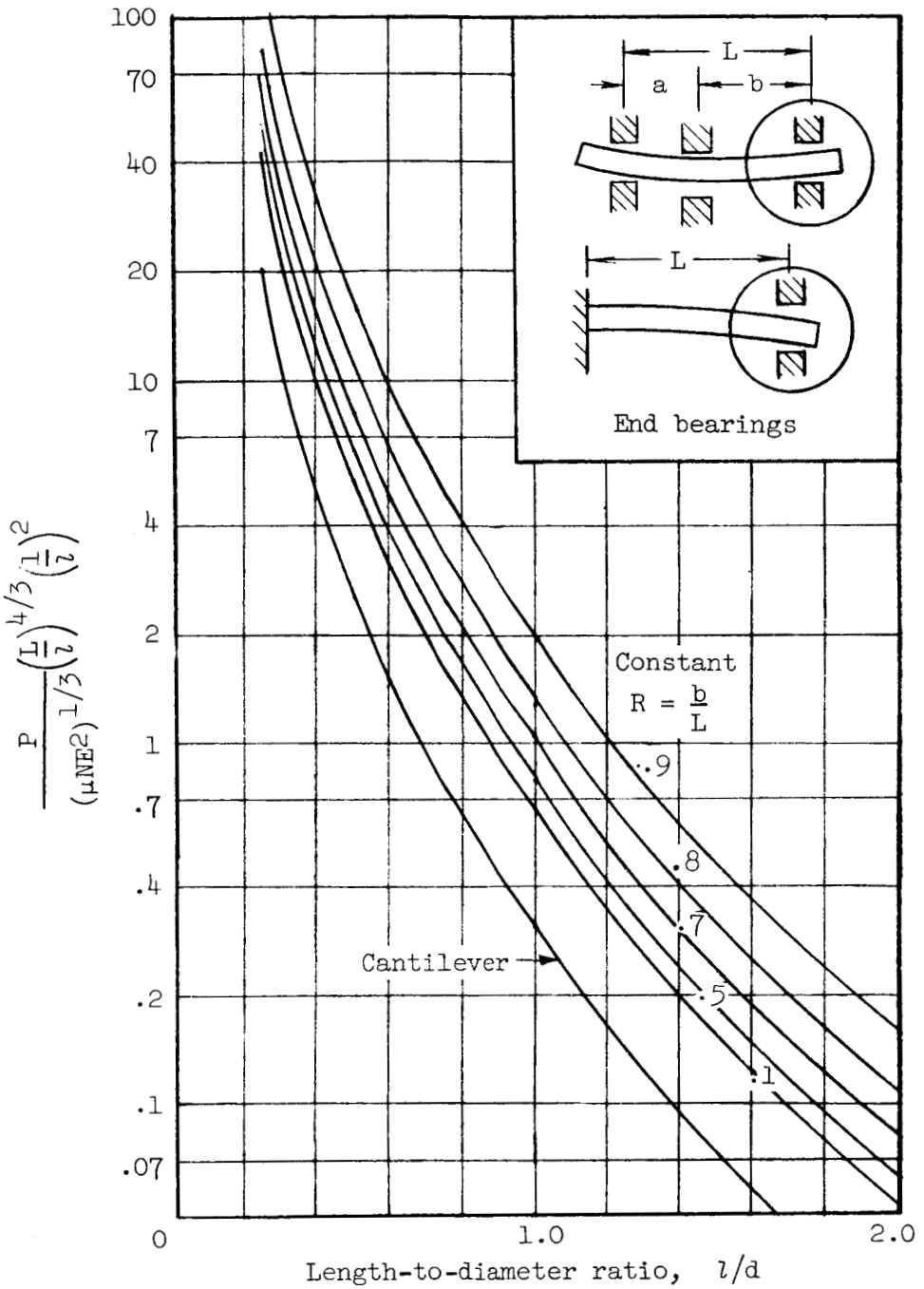

(a) Based on short-bearing approximation, $f(n) = 0.718$.

Figure 11.- Total load capacity of end bearings against bearing diameter at impending contact of surfaces due to shaft deflection.

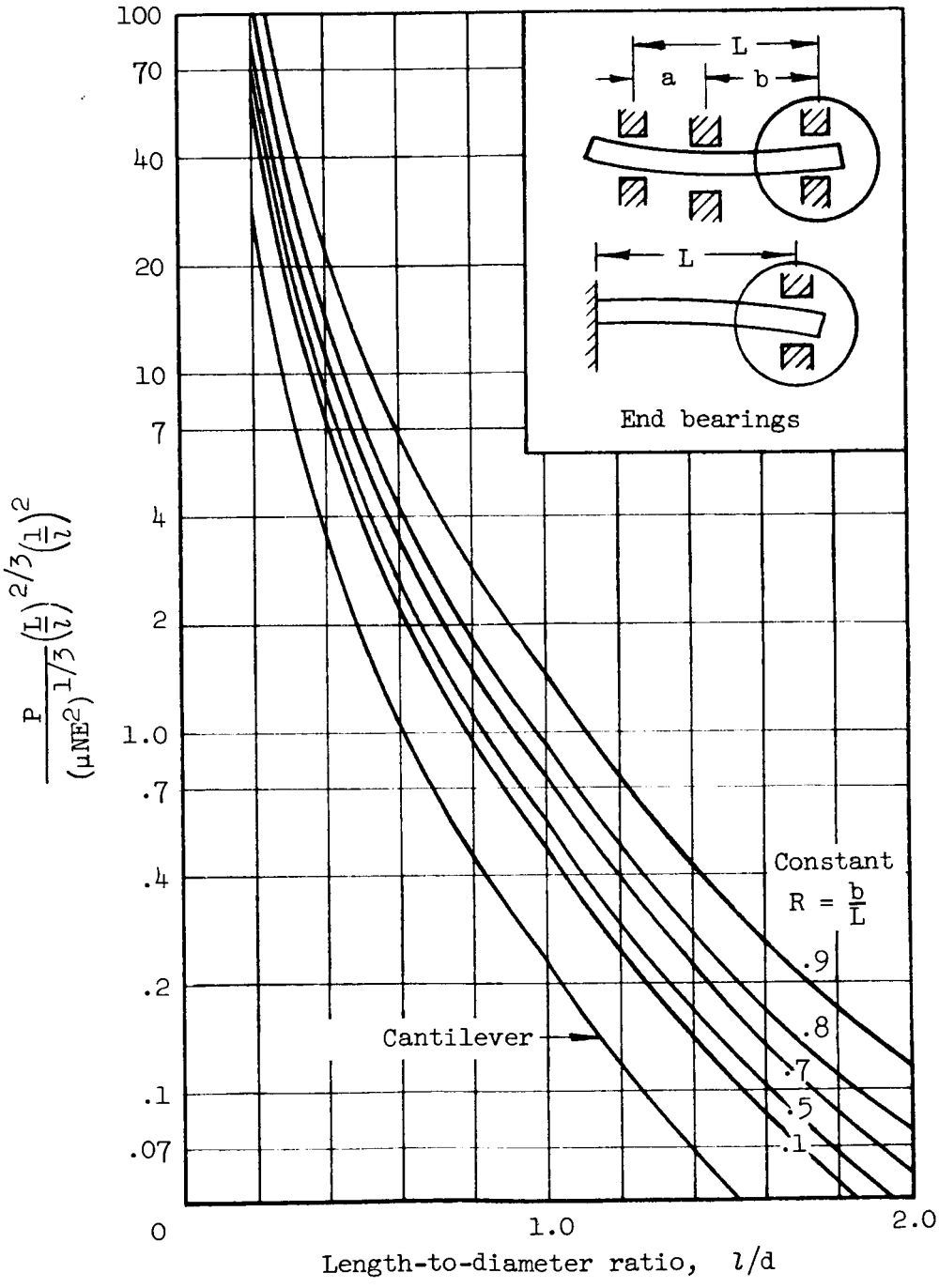

(b) Based on experimental data, f(n) = 0.30.

Figure 11.- Concluded.

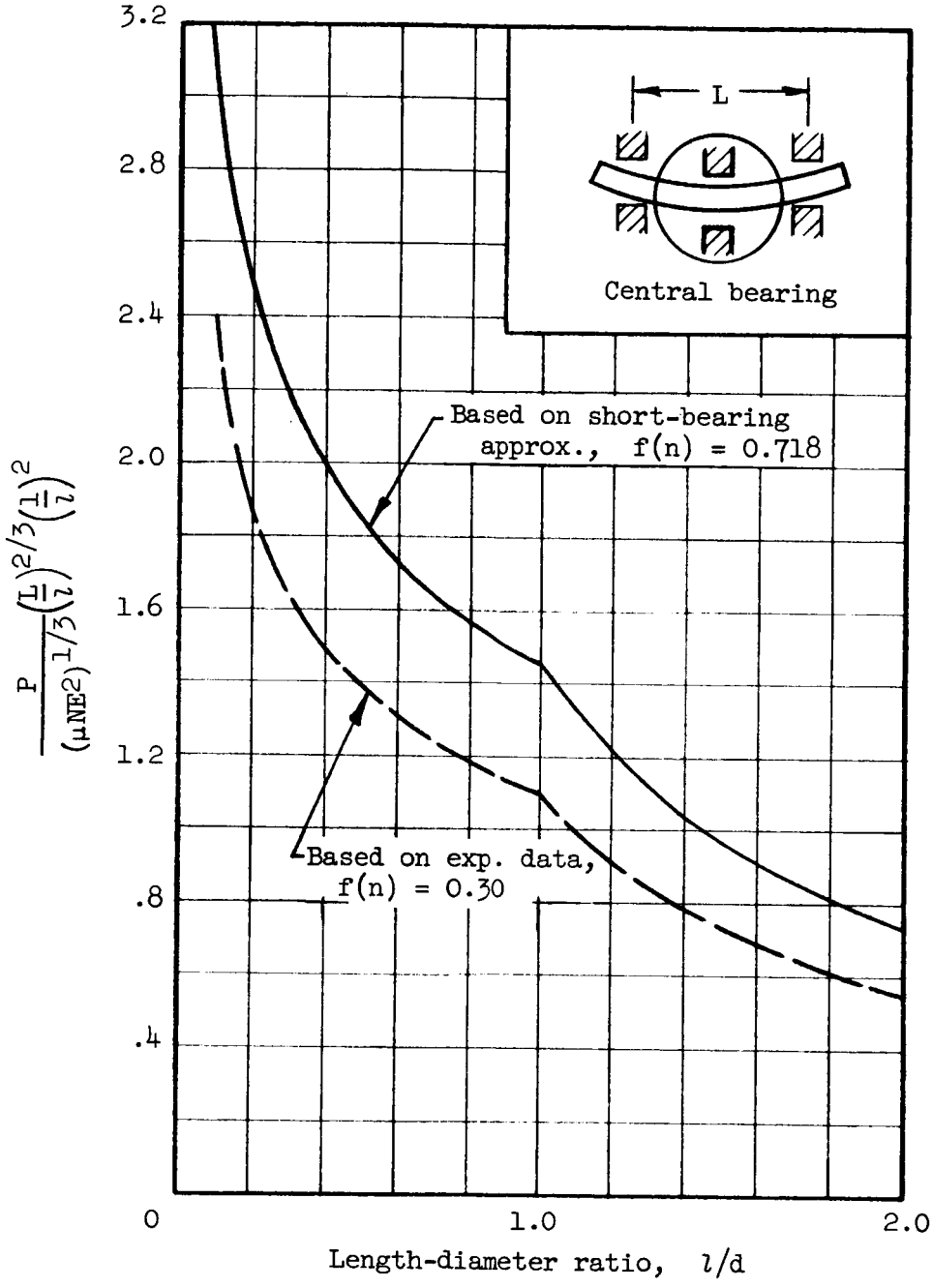

Figure 12.- Total load capacity of central bearings against bearing length at impending contact of surfaces due to shaft deflection.

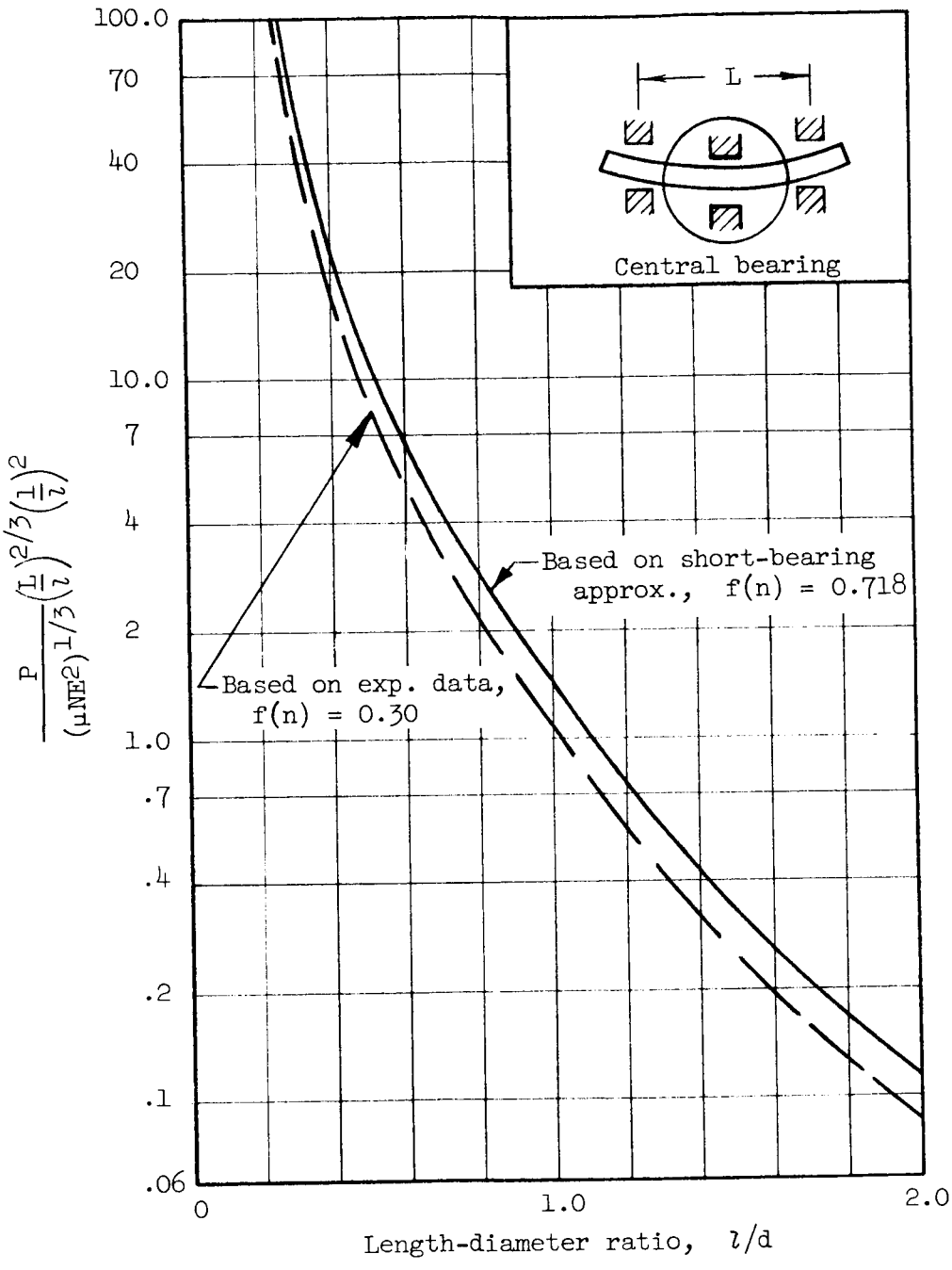

Figure 13.- Total load capacity of central bearings against bearing diameter at impending contact of surfaces due to shaft deflection.

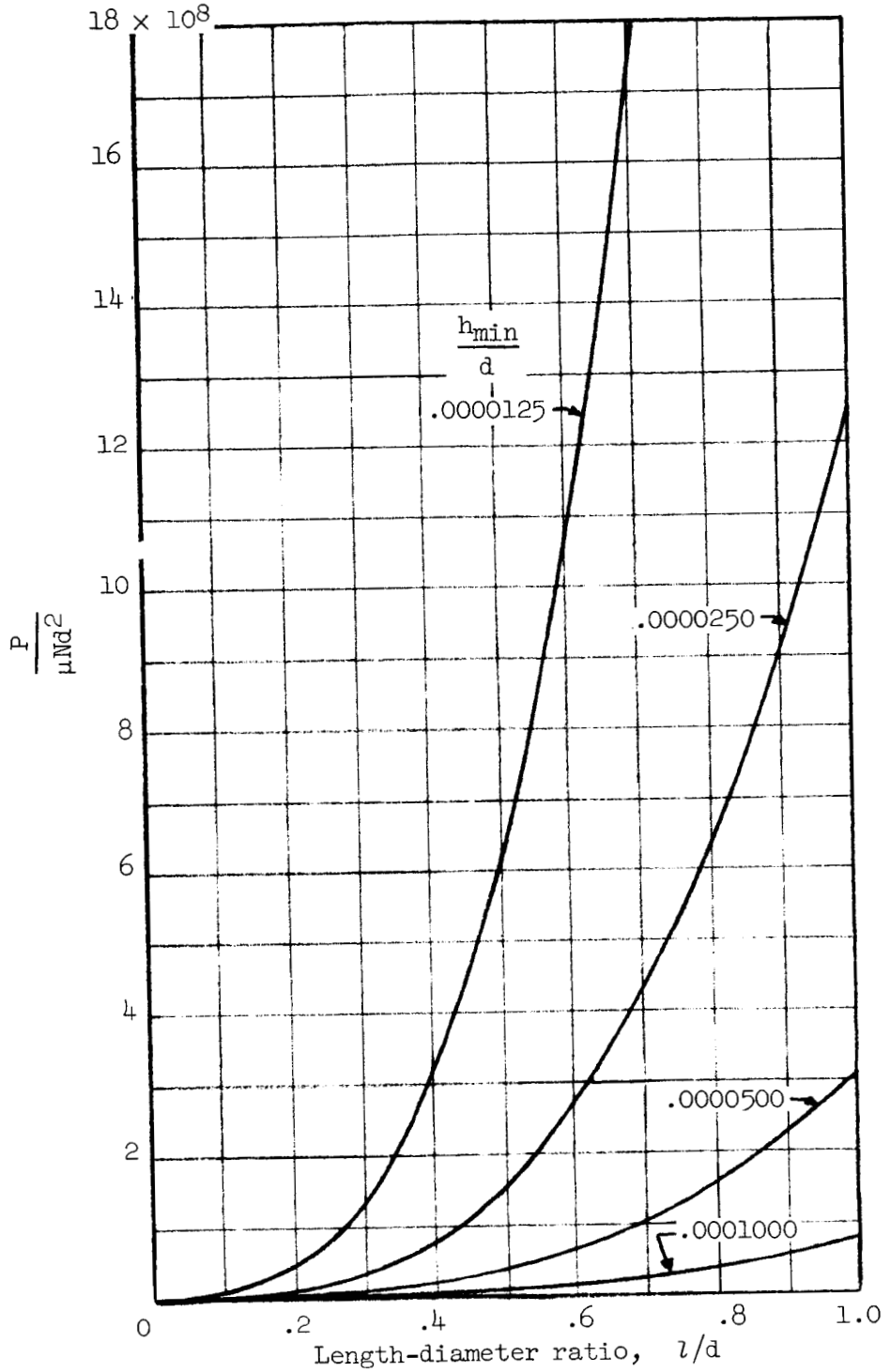

Figure 14.- Hydrodynamic total load capacity against film thickness ratio and length-diameter ratio neglecting deflection. (For $l/d \leqq 1$, h_{min} is sum of surface roughnesses at impending contact of surface asperities.)

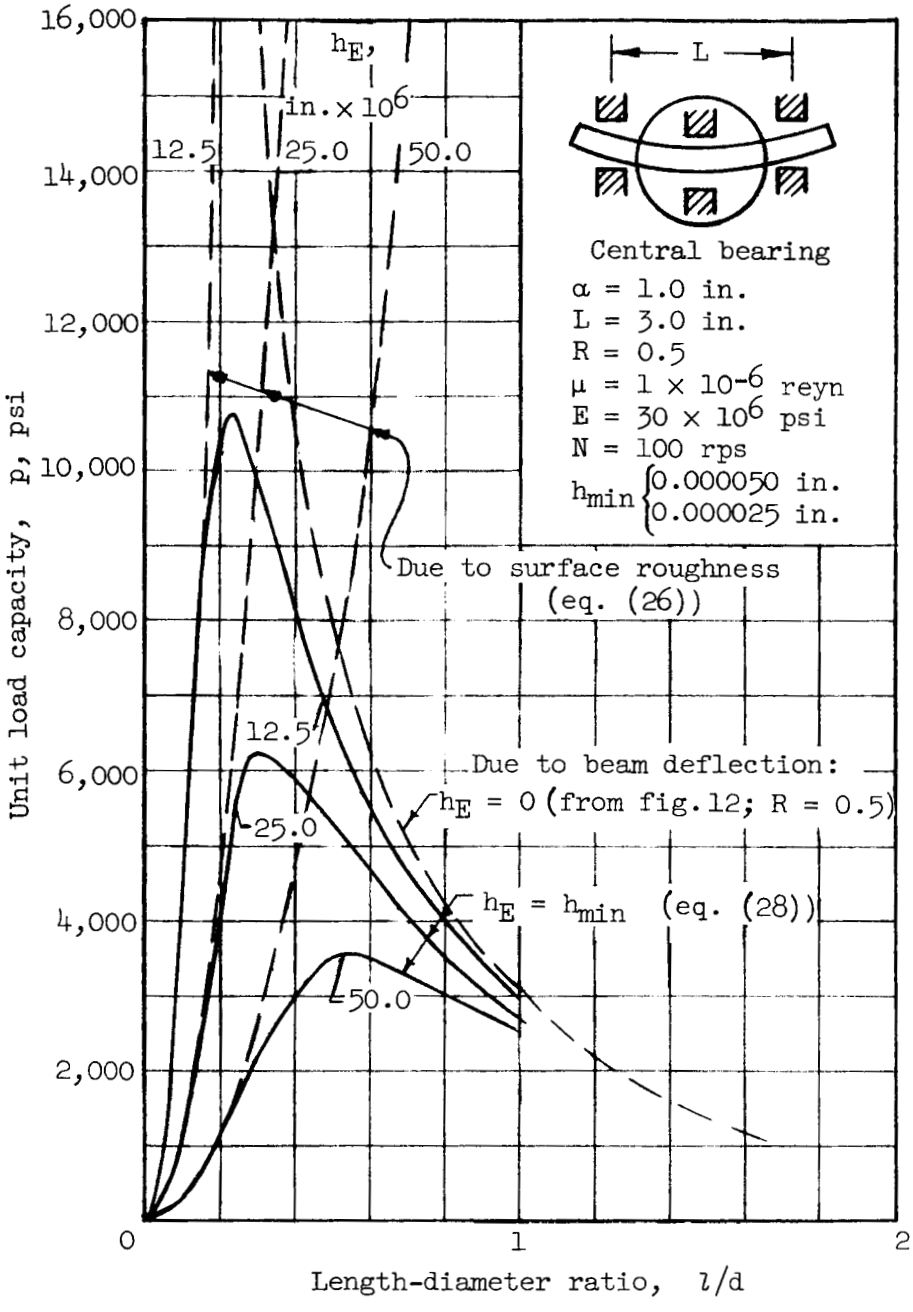

(a) Central bearing.

Figure 15.- Unit load capacity of bearing against bearing length for a given design situation. Curves are analytically determined for impending contact of surfaces due to both shaft deflection and surface roughness. (Compare with experimental curve of figure 17.)

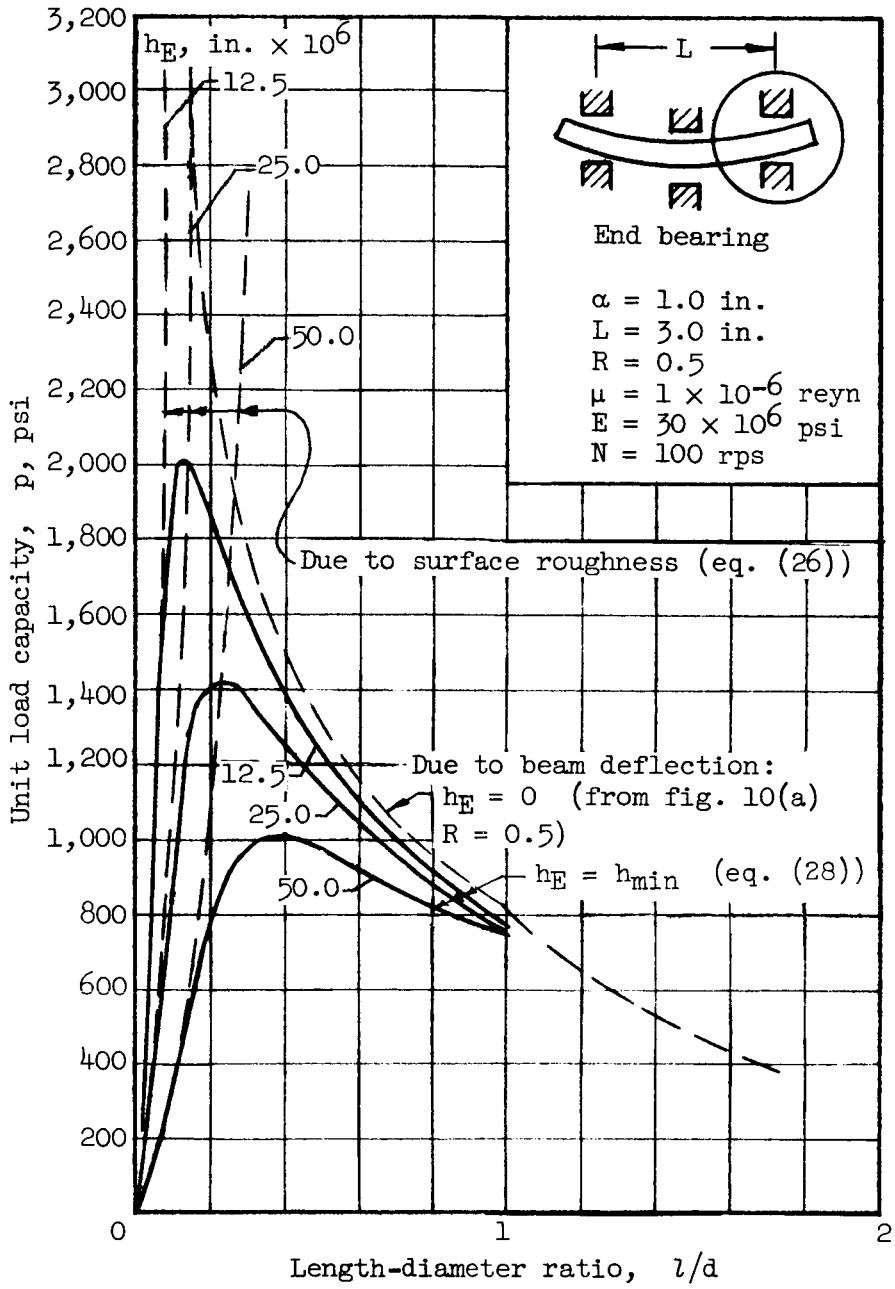

(b) End bearing.

Figure 15.- Concluded.

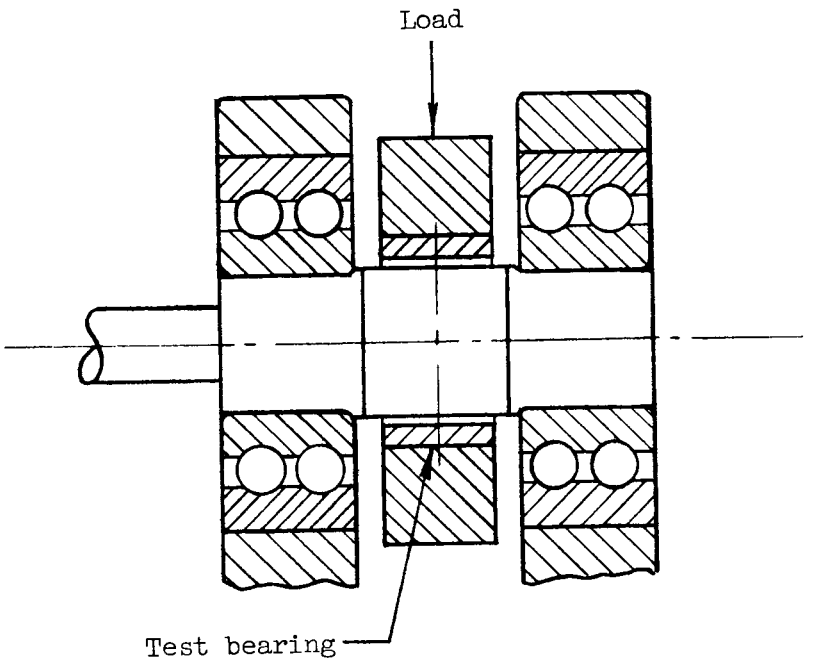

Figure 16.- Bearing test arrangement used by Battelle Memorial Institute (refs. 8 and 9) to determine load capacities of central bearings by experiment.

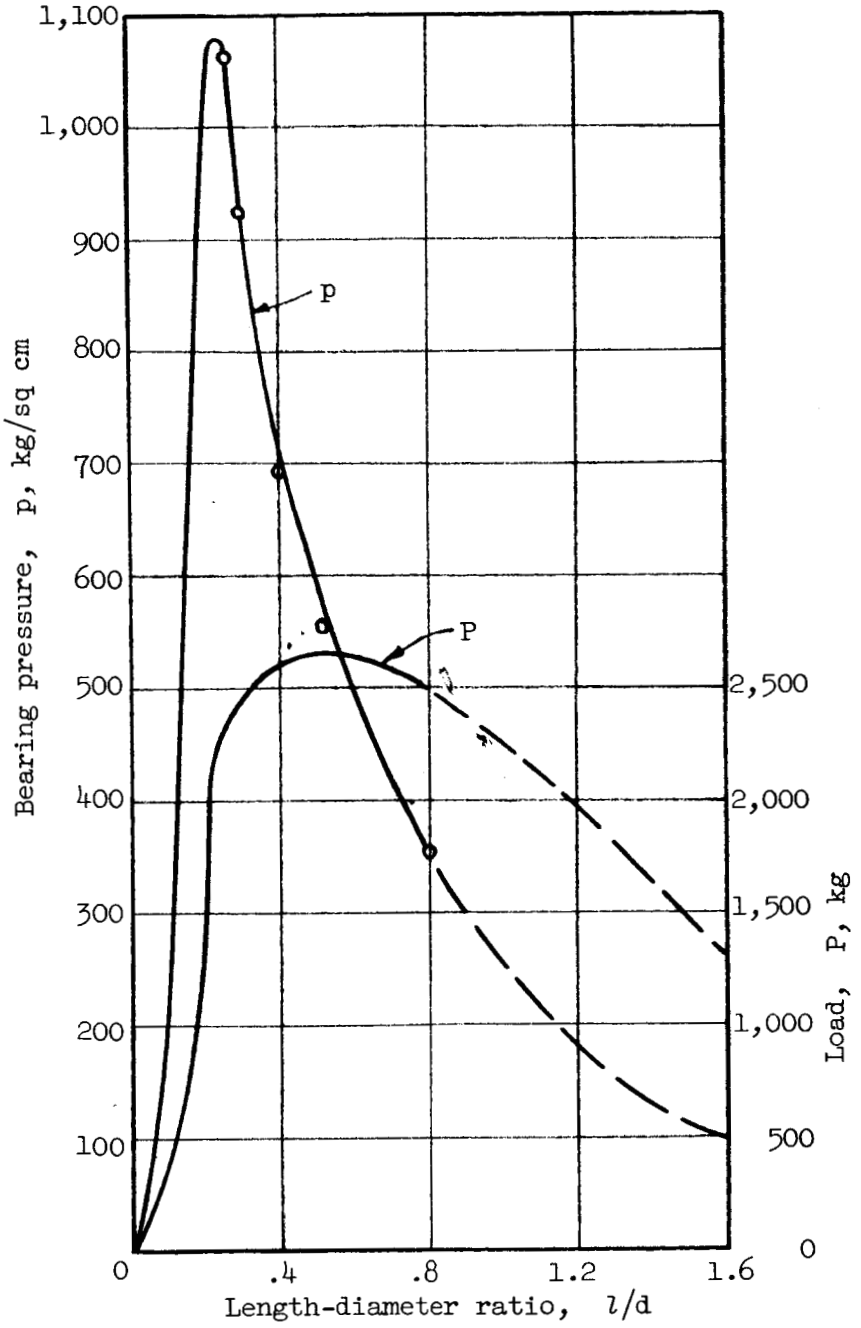

Figure 17.- Curves of bearing load capacity against l/d determined from experiment (ref. 6). Compare with analytical curves of figures 15(a), 15(b), and 18(b).

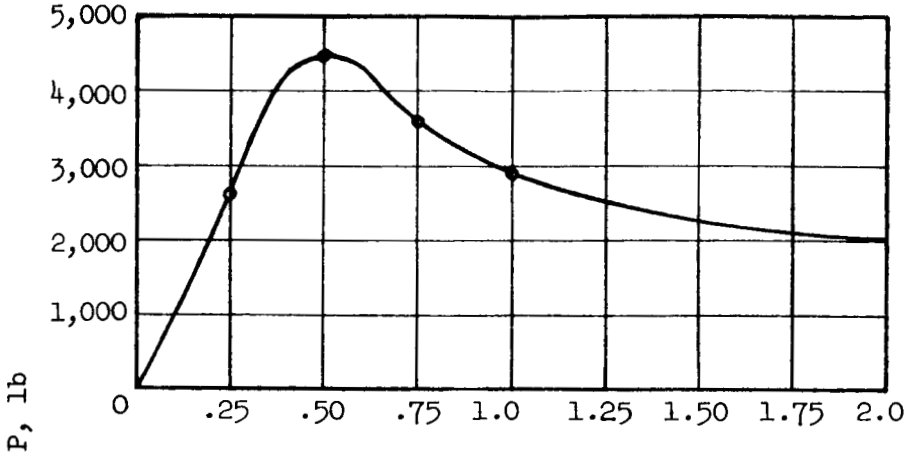

(a) Experimental curve from reference 7.

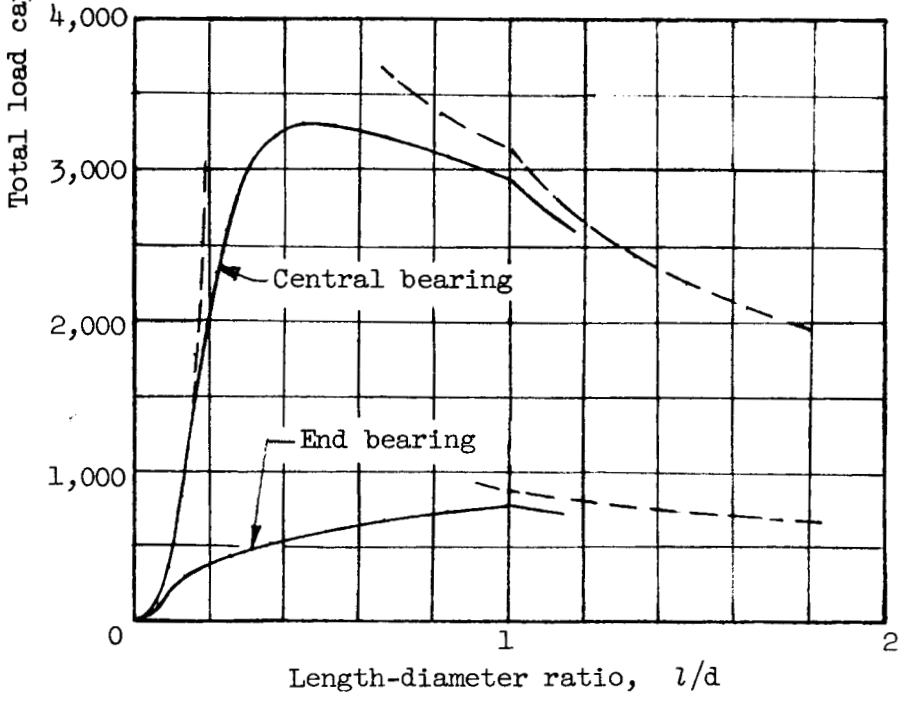

(b) Analytical curves. Compare with experimental curve in figure 17. (See fig. 15 for data and unit loads; h_E = 0.0000125 in.)

Figure 18.- Total load capacity of bearings against l/d.